Available online at www.sciencedirect.com
ScienceDirect
Engineering Structures 30 (2008) 1319–1334
ENGINEERING STRUCTURES
www.elsevier.com/locate/engstruct

Quadruply coupled linear free vibrations of thin-walled beams with a generic open section

Hong Hu Chen, Kuo Mo Hsiao*

Department of Mechanical Engineering, National Chiao Tung University, 1001 Ta Hsueh Road, Hsinchu, Taiwan

Received 10 February 2007; received in revised form 6 July 2007; accepted 10 July 2007
Available online 5 September 2007

Abstract

The coupled vibration of thin-walled beams with a generic open section induced by the boundary conditions is investigated using the finite element method. If the axial displacement of the pin end is restrained at another point rather than the centroid of the asymmetric cross section, the axial vibration, two bending vibrations, and torsional vibration may be all coupled. The element developed here has two nodes with seven degrees of freedom per node. The shear center axis is chosen to be the reference axis and the element nodes are chosen to be located at the shear centers of the end cross sections of the beam element. Different sets of element nodal degrees of freedom corresponding to different pin ends are considered here. The relation between element matrices referred to different sets of element nodal degrees of freedom is derived.

Numerical examples are presented to demonstrate the accuracy of the proposed method and to investigate the effects of different pin ends on the coupled vibrations of the thin-wall beam.

Keywords: Natural frequency; Coupled vibration; Thin-walled beam; Finite element method

1. Introduction

Thin-walled beams of open cross section are widely used in structural design. The vibration characteristics are of fundamental importance in the design of thin-walled structures. In general, the shear center and the centroid of cross section for monosymmetric or asymmetric thin-walled beams are not coincident. Thus, the bending and torsional vibrations are coupled. The doubly coupled bending–torsional vibrations of monosymmetric beams and the triply coupled bending–bending–torsional vibration of asymmetric beams have been investigated by several authors [1–24] in recent years. Recently, in [25] the influence of shear deformation over the natural frequencies is investigated for the Timoshenko thin-walled beam with arbitrary open cross section. In the literature, the axial vibration is considered to be uncoupled from the bending and torsional vibrations and can be analyzed independently. However, for the axial pin end, this consideration may only be correct in the case that the axial displacement is restrained at the centroid of the cross section. If the axial displacement of the pin end is not restrained at a point in the longitudinal plane of symmetry of the monosymmetric cross section or not restrained at the centroid of the asymmetric cross section, the axial vibration, two bending vibrations, and torsional vibration may be all coupled. Coupled vibration of that kind is induced by the boundary conditions and will be called quadruply coupled vibration in the study. To the authors' knowledge, the quadruply coupled vibration induced by the boundary conditions has not been reported in the literature. The object of this paper is to investigate the quadruply coupled vibration of thin-walled beams with a generic open section induced by the boundary conditions using the finite element method.

In beam theories, it is assumed that the beam cross section does not deform in its own plane. Thus, the relation between displacements corresponding to different points on the cross section of the beam can be determined using the kinematics of a rigid body. To describe the deformation of the beam, the axial displacement and lateral displacements of the beam may be defined at different reference axes. The equations of motion of the beam corresponding to different sets of reference axes

* Corresponding author. Tel.: +886 3 5712121 55107; fax: +886 3 5720634.
E-mail address: kmhsiao@mail.nctu.edu.tw (K.M. Hsiao).

0141-0296/$ - see front matter © 2007 Elsevier Ltd. All rights reserved.
doi:10.1016/j.engstruct.2007.07.004

are equivalent. Traditionally, two reference axes are used for the linear analysis of thin walled beams with a generic open cross section. The axial force and bending moments are defined at the centroid and the shear force, twist moment and bimoment are defined at the shear center, which can uncouple the linear equilibrium equations to the largest extent. However, it is more convenient to use one reference axis to describe the motion of the beam for finite element formulations. The stiffness matrices of the beam element referred to different nodal degrees of freedom are equivalent, and can be transformed to each other using standard procedures. However, to describe the boundary conditions correctly, the restrained nodal degrees of freedom at boundaries and the corresponding nodal degrees of freedom of the beam element should be identical or equivalent. In [17], the centroid axis is used as the reference axis. In [26], the shear center axis is chosen to be the reference axis and a finite element formulation is proposed for the geometrical nonlinear analysis of a thin-walled beam with a generic open section. The beam element proposed in [26] has two nodes with seven degrees of freedom per node. Element deformations and element equations were defined in terms of element coordinates. The element deformations are determined by the rotation of the element cross section coordinates, which are rigidly tied to the element cross section, relative to the element coordinate system. The out-of-plane warping of the cross section was assumed to be the product of the twist rate of the beam element and the Saint Venant warping function for a prismatic beam of the same cross section. The element nodal forces are derived by the virtual work principle and the consistent second-order linearization of the fully geometrically nonlinear beam theory. It seems that the kinematics of the beam element proposed in [26] can be linearized and extended for the linear dynamic analysis of the beam structures we discuss. Thus, the formulation of the beam element presented in [26] is linearized and employed here.

Following [26], the shear center axis is chosen to be the reference axis and the element nodes are chosen to be located at the shear centers of the end cross sections of the beam element. The element deformation and inertial nodal forces are systematically derived using a consistent linearization of exact kinematics of the Euler beam, the d'Alembert principle, and the virtual work principle. The element stiffness matrix and mass matrix are obtained by differentiating the element deformation nodal force vector and the element inertial nodal force vector with respect to the element nodal parameters and their second time derivatives, respectively. As mentioned above, to describe the boundary conditions correctly, the restrained nodal degrees of freedom and the corresponding nodal degrees of freedom of the beam element should be identical or equivalent. Different sets of element nodal degrees of freedom corresponding to different pin ends are considered here. The transformation between the element matrices corresponding to different sets of element nodal degrees of freedom is derived using the kinematic relation between different sets of element nodal degrees of freedom.

The subspace iteration method is employed for the solution of the generalized eigenvalue problem. Numerical examples are studied for a thin-walled beam with different boundary conditions to demonstrate the accuracy of the proposed method and to investigate the effects of different boundary conditions on the natural frequencies and vibration modes of a thin-wall beam with a generic open section.

2. Finite element formulation

The kinematics of thebeam element proposed in [26] is linearized and employed here. Only a brief description for the kinematics of this beam element is given here. A more detailed description may be obtained from [26]. The element deformation and inertial nodal forces of the linear beam element are derived using the d'Alembert principle and the virtual work principle.

2.1. Basic assumptions

The following assumptions are made in the derivation of the behavior of the thin-walled beam element with a generic open section.

(1) The beam is prismatic and slender, and the Euler–Bernoulli hypothesis is valid if the out-of-plane warping of the cross section is excluded.
(2) When the longitudinal normal strain at the centroidal axis relevant to the twist about the shear center axis is excluded, the unit extension of the centroid axis of the beam element corresponding to the rest of longitudinal normal strain is uniform.
(3) The cross section of the beam element does not deform in its own plane and strains within this cross section can be neglected.
(4) The out-of-plane warping of the cross section is the product of the twist rate of the beam element and the Saint Venant warping function for a prismatic thin walled beam of the same cross section.
(5) The material is homogeneous, isotropic, and linear elastic.

In this study, Prandtl's membrane analogy and the Saint Venant torsion theory [26,27] are used to obtain an approximate Saint Venant warping function for a prismatic thin walled beam. However, if the accurate warping function for beams of arbitrary cross-section is required, the method proposed in [28,29] may be used.

2.2. Coordinate systems

In order to describe the system, we define three sets of right handed rectangular Cartesian coordinate systems:

(1) A fixed global set of coordinates, X_i^G $(i = 1, 2, 3)$ (see Fig. 1); the nodal coordinates, nodal displacements and rotations, nodal velocity and angular velocity, nodal acceleration and angular acceleration, and the stiffness matrix and the mass matrix of the system are defined in these coordinates.

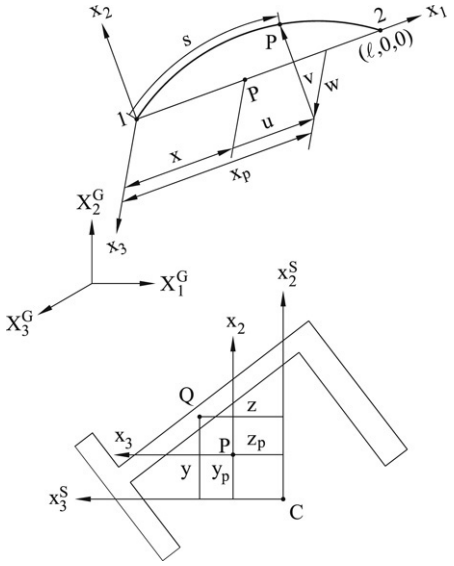

Fig. 1. Coordinate systems.

(2) Element cross section coordinates, x_i^S ($i = 1, 2, 3$) (see Fig. 1); a set of element cross section coordinates is associated with each cross section of the beam element. The origin of this coordinate system is rigidly tied to the *centroid* of the cross section. The x_1^S axis is chosen to coincide with the *normal of the unwarped* cross section and the x_2^S and x_3^S axes are chosen to be the *principal centroidal axes* of the cross section.

(3) Element coordinates; x_i ($i = 1, 2, 3$) (see Fig. 1), a set of element coordinates is associated with each element. The origin of this coordinate system is located at node 1, and the x_1 axis is chosen to pass through the two end nodes (*shear centers of end sections*) of the element; the directions of the x_2 and x_3 axes are chosen to coincide with the directions of the principal centroidal axes of the cross section in the undeformed state. The deformations, deformation nodal forces, inertial nodal forces, stiffness matrix, and mass matrix of the elements are defined in terms of these coordinates. In this paper, the element deformations are determined by the rotation of element cross section coordinate systems relative to this coordinate system.

2.3. Kinematics of the beam element

The deformations of the beam element are described in the element coordinate system. Here, the shear center axis is chosen to be the reference axis and the element nodes are chosen to be located at the shear centers of the end cross sections of the beam element. Let Q (Fig. 1) be an arbitrary point in the beam element, and P be the point corresponding to Q on the shear center axis. The position vector of point Q in the undeformed and deformed configurations may be expressed as:

$$\mathbf{r}_0 = x\mathbf{e}_1 + (y - y_p)\mathbf{e}_2 + (z - z_p)\mathbf{e}_3 \tag{1}$$

and

$$\mathbf{r} = x_p(x,t)\mathbf{e}_1 + v(x,t)\mathbf{e}_2 + w(x,t)\mathbf{e}_3 + \theta_{1,x}\omega\mathbf{e}_1^S + (y - y_p)\mathbf{e}_2^S + (z - z_p)\mathbf{e}_3^S = r_i\mathbf{e}_i \tag{2}$$

$$x_p(x,t) = x + u(x,t)$$

where y_p and z_p, and y and z are the x_2^S and x_3^S coordinates of point P and Q referred to the element cross section coordinates, respectively, $u(x,t)$, $v(x,t)$, and $w(x,t)$ are the x_i ($i = 1, 2, 3$) components of the displacement vector of point P referred to the element coordinates in the deformed configuration, respectively, $\theta_1 = \theta_1(x,t)$ and $\theta_{1,x} = \partial\theta_1/\partial x$ are the twist angle and the twist rate about the shear center axis, respectively, $\omega = \omega(y,z)$ is the Saint Venant warping function for a prismatic beam of the same cross section, and $\mathbf{e}_i$ and $\mathbf{e}_i^S$ ($i = 1, 2, 3$) denote the unit vectors associated with the x_i and x_i^S axes, respectively. Note that the directions of $\mathbf{e}_i$ and $\mathbf{e}_i^S$ are the same in the undeformed state. The orientations of triad $\mathbf{e}_i^S$ in the deformed state are assumed to be determined by two successive rotations of the triad $\mathbf{e}_i$ about an axis perpendicular to the shear center axis and about the shear center axis [26]. The relation between the vectors $\mathbf{e}_i$ and $\mathbf{e}_i^S$ ($i = 1, 2, 3$) in the element coordinate system may be expressed by [30]

$$\mathbf{e}_i^S = \mathbf{R}\mathbf{e}_i \tag{3}$$

where $\mathbf{R}$ is a rotation matrix. The rotation matrix $\mathbf{R}$ is determined by θ_1 and

$$\theta_2 = -\frac{\partial w(x,t)}{\partial s} = -\frac{\partial w(x,t)}{\partial x}\frac{\partial x}{\partial s} = -\frac{w'}{1+\varepsilon_o},$$

$$\theta_3 = \frac{\partial v(x,t)}{\partial s} = \frac{\partial v(x,t)}{\partial x}\frac{\partial x}{\partial s} = \frac{v'}{1+\varepsilon_o} \tag{4}$$

$$\varepsilon_o = \frac{\partial s}{\partial x} - 1 \tag{5}$$

in which ε_o is the unit extension of the shear center axis and s is the arc length of the deformed shear center axis measured from node 1 to point P. In this paper, the symbol ( ) denotes $(\,)_{,x} = \partial(\,)/\partial x$.

In this study, the θ_i are called rotation parameters. Let $\boldsymbol{\theta} = \{\theta_1, \theta_2, \theta_3\}$ be the column matrix of rotation parameters, $\delta\boldsymbol{\theta}$ be the variation of $\boldsymbol{\theta}$, and $\delta\boldsymbol{\varphi} = \{\delta\varphi_1, \delta\varphi_2, \delta\varphi_3\}$ be the column matrix of $\delta\varphi_i$ ($i = 1, 2, 3$), infinitesimal rotations about x_i axes. The triad $\mathbf{e}_i^S$ ($i = 1, 2, 3$) corresponding to $\boldsymbol{\theta}$ may be rotated by a $\delta\boldsymbol{\varphi}$ to reach their new positions corresponding to $\boldsymbol{\theta} + \delta\boldsymbol{\theta}$ [30]. In the undeformed state, $\theta_1 = \theta_2 = \theta_3 = 0$ and $\varepsilon_o = 0$, the relationship between $\delta\boldsymbol{\theta}$ and $\delta\boldsymbol{\varphi}$ given in [30] may be degenerated to

$$\delta\boldsymbol{\theta} = \delta\boldsymbol{\varphi} \tag{6}$$

$$\delta\theta_1 = \delta\varphi_1, \qquad \delta\theta_2 = -\delta w' = \delta\varphi_2, \qquad \delta\theta_3 = \delta v' = \delta\varphi_3.$$

Similarly, the time derivatives of $\boldsymbol{\theta}$ may be degenerated to [31]

$$\dot{\boldsymbol{\theta}} = \boldsymbol{\omega} \tag{7}$$

$$\dot{\theta}_1 = \omega_1, \qquad \dot{\theta}_2 = -\dot{w}' = \omega_2, \qquad \dot{\theta}_3 = \dot{v}' = \omega_3$$

and

$$\ddot{\boldsymbol{\theta}} = \dot{\boldsymbol{\omega}} \tag{8}$$

$$\ddot{\theta}_1 = \dot{\omega}_1, \qquad \ddot{\theta}_2 = -\ddot{w}' = \dot{\omega}_2, \qquad \ddot{\theta}_3 = \ddot{v}' = \dot{\omega}_3$$

where $\boldsymbol{\omega}$ is the angular velocity vector, $\dot{\boldsymbol{\omega}}$ is the angular acceleration vector, and ω_i and $\dot{\omega}_i$ $(i = 1, 2, 3)$ are x_i components of $\boldsymbol{\omega}$ and $\dot{\boldsymbol{\omega}}$, respectively. In this paper, the symbol $\dot{(\,)}$ denotes the time derivative.

The relationship among $x_p(x,t)$, $v(x,t)$, $w(x,t)$ in Eq. (2) may be given as

$$x_p(x,t) = u_1 + \int_0^x [(1+\varepsilon_o)^2 - v_{,x}^2 - w_{,x}^2]^{1/2} \mathrm{d}x \tag{9}$$

where u_1 is the displacement of node 1 in the x_1 direction.

Making use of Eq. (9), one obtains

$$\begin{aligned} \ell &= L + u_2 - u_1 = x_p(L,t) - x_p(0,t) \\ &= \int_0^L [(1+\varepsilon_o)^2 - v_{,x}^2 - w_{,x}^2]^{1/2} \mathrm{d}x \end{aligned} \tag{10}$$

in which ℓ is the chord length of the deformed shear center axis of the beam element, L is the length of the undeformed beam axis, and u_2 is the displacement of node 2 in the x_1 direction.

Here, the lateral deflections of the shear center axis, $v(x,t)$ and $w(x,t)$, and the rotation about the shear center axis, $\theta_1(x,t)$, are assumed to be the Hermitian polynomials of x. $v(x,t)$, $w(x,t)$ and $\theta_1(x,t)$ may be expressed by

$$\begin{aligned} &v(x,t) = \mathbf{N}_b^t \mathbf{u}_b, \qquad w(x,t) = \mathbf{N}_c^t \mathbf{u}_c, \\ &\theta_1(x,t) = \mathbf{N}_d^t \mathbf{u}_d \end{aligned} \tag{11}$$

$$\begin{aligned} &\mathbf{u}_b = \{v_1, v_1', v_2, v_2'\}, \qquad \mathbf{u}_c = \{w_1, -w_1', w_2, -w_2'\}, \\ &\mathbf{u}_d = \{\theta_{11}, \beta_1, \theta_{12}, \beta_2\} \end{aligned} \tag{12}$$

where v_j and w_j $(j = 1, 2)$ are nodal values of v and w at nodes j, respectively, v_j' and w_j' $(j = 1, 2)$ are nodal values of $v_{,x}$ and $w_{,x}$ at nodes j, respectively, and θ_{1j} and β_j $(j = 1, 2)$ are nodal values of θ_1, $\theta_{1,x}$ at nodes j, respectively.

The axial displacements of the shear center axis may be determined from the lateral deflections and the unit extension of the shear center axis using Eq. (9).

If x, y and z in Eq. (1) are regarded as the Lagrangian coordinates, the Green strain ε_{11}, ε_{12} and ε_{13} are given by [32]

$$\begin{aligned} &\varepsilon_{11} = \frac{1}{2}(\mathbf{r}_{,x}^t \mathbf{r}_{,x} - 1), \qquad \varepsilon_{12} = \frac{1}{2}\mathbf{r}_{,x}^t \mathbf{r}_{,y}, \\ &\varepsilon_{13} = \frac{1}{2}\mathbf{r}_{,x}^t \mathbf{r}_{,z}. \end{aligned} \tag{13}$$

Substituting Eqs. (2)–(5) into Eq. (13), making use of assumption (2), Eq. (13), and retaining all terms up to the first order yields [26]

$$\varepsilon_{11} = \varepsilon_c - y v_{,xx} - z w_{,xx} + \omega \theta_{1,xx} \tag{14a}$$

$$\varepsilon_{12} = \frac{1}{2}[\omega_{,y} - (z - z_p)]\theta_{1,x} \tag{14b}$$

$$\varepsilon_{13} = \frac{1}{2}[\omega_{,z} + (y - y_p)]\theta_{1,x} \tag{14c}$$

$$\varepsilon_o = \varepsilon_c - y_p v_{,xx} - z_p w_{,xx} \tag{15}$$

$$\varepsilon_c = \frac{u_2 - u_1}{L} + \frac{y_p}{L}(v_2' - v_1') + \frac{z_p}{L}(w_2' - w_1'). \tag{16}$$

2.4. Element nodal force vector

The element proposed here has two nodes with seven degrees of freedom per node. The element nodal force is obtained from the d'Alembert principle and the virtual work principle in the element coordinates. The virtual work principle requires that

$$\delta W_E = \delta W_I \tag{17a}$$

$$\delta W_E = \delta \mathbf{u}_a^t \mathbf{f}_a + \delta \mathbf{u}_b^t \mathbf{f}_b + \delta \mathbf{u}_c^t \mathbf{f}_c + \delta \mathbf{u}_d^t \mathbf{f}_d \tag{17b}$$

$$\begin{aligned} \delta W_I = &\int_V (\sigma_{11}\delta\varepsilon_{11} + 2\sigma_{12}\delta\varepsilon_{12} + 2\sigma_{13}\delta\varepsilon_{13})\mathrm{d}V \\ &+ \int_V \rho \delta \mathbf{r}^t \ddot{\mathbf{r}} \mathrm{d}V \end{aligned} \tag{17c}$$

$$\delta \mathbf{u}_a = \{\delta u_1, \delta u_2\} \tag{18}$$

$$\mathbf{f}_a = \mathbf{f}_a^d + \mathbf{f}_a^I = \{f_{11}, f_{12}\} \tag{19a}$$

$$\mathbf{f}_b = \mathbf{f}_b^d + \mathbf{f}_b^I = \{f_{21}, m_{31}, f_{22}, m_{32}\} \tag{19b}$$

$$\mathbf{f}_c = \mathbf{f}_c^d + \mathbf{f}_c^I = \{f_{31}, m_{21}, f_{32}, m_{22}\} \tag{19c}$$

$$\mathbf{f}_d = \mathbf{f}_d^d + \mathbf{f}_d^I = \{m_{11}, B_1, m_{12}, B_2\} \tag{19d}$$

where δW_E is the virtual work of the external force, δW_I is the virtual work of the internal stress, $\delta \mathbf{u}_j$ $(j = b, c, d)$ are variations of $\mathbf{u}_j$ in Eq. (12), V is the volume of the undeformed beam, $\delta\varepsilon_{1j}$ $(j = 1, 2, 3)$ are the variations of ε_{1j} in Eqs. (14a)–(14c), respectively. σ_{1j} $(j = 1, 2, 3)$ are the second Piola–Kirchhoff stresses, ρ is the density, $\delta\mathbf{r}$ and $\ddot{\mathbf{r}}$ are the variation and the second-time derivative of $\mathbf{r}$ in Eq. (2), respectively. $\mathbf{f}_j^d$ and $\mathbf{f}_j^I$ $(j = a, b, c, d)$ are element deformation nodal forces and element inertial nodal forces, respectively. f_{ij} and m_{ij} $(i = 1, 2, 3,\ j = 1, 2)$ are forces in the x_i directions at nodes j and moments about the x_i axes at nodes j, respectively. B_j $(j = 1, 2)$ are the bimoments at nodes j.

The constitutive equations used here are $\sigma_{11} = E\varepsilon_{11}$, $\sigma_{12} = 2G\varepsilon_{12}$, and $\sigma_{13} = 2G\varepsilon_{13}$, where E is the Young's modulus and G is the shear modulus.

For linear analysis, only the first order terms of nodal parameters and their derivatives with respect to x and t in the element internal nodal forces are retained by consistent linearization.

From Eqs. (14)–(16), $\delta\varepsilon_{1j}$ $(j = 1, 2, 3)$ in Eq. (17c) may be expressed by

$$\delta\varepsilon_{11} = \delta\varepsilon_c - y\delta v_{,xx} - z\delta w_{,xx} + \omega\delta\theta_{1,xx} \tag{20a}$$

$$\delta\varepsilon_{12} = \frac{1}{2}[\omega_{,y} - (z - z_p)]\delta\theta_{1,x} \tag{20b}$$

$$\delta\varepsilon_{13} = \frac{1}{2}[\omega_{,z} + (y - y_p)]\delta\theta_{1,x} \tag{20c}$$

$$\delta\varepsilon_c = \frac{\delta u_2 - \delta u_1}{L} + \frac{y_p}{L}(\delta v_2' - \delta v_1') + \frac{z_p}{L}(\delta w_2' - \delta w_1'). \tag{21}$$

From Eqs. (2) and (6)–(11) and using consistent linearization, $\delta\mathbf{r}$ and $\ddot{\mathbf{r}}$ given in Eq. (17c) may be expressed by

$$\delta r_1 = \delta x_p - (y - y_p)\delta v_{,x} - (z - z_p)\delta w_{,x} + \delta\theta_{1,x}\omega \tag{22a}$$

$$\delta r_2 = \delta v - (z - z_p)\delta\theta_1 \tag{22b}$$

$$\delta r_3 = \delta w + (y - y_p)\delta\theta_1 \tag{22c}$$

$$\delta x_p = \delta u_1 + x\delta\varepsilon_c - y_p(\delta v' - \delta v_1') - z_p(\delta w' - \delta w_1') \tag{23}$$

$$\ddot{r}_1 = \ddot{x}_p - (y - y_p)\ddot{v}_{,x} - (z - z_p)\ddot{w}_{,x} + \ddot{\theta}_{1,x}\omega \tag{24a}$$

$$\ddot{r}_2 = \ddot{v} - (z - z_p)\ddot{\theta}_1 \tag{24b}$$

$$\ddot{r}_3 = \ddot{w} + (y - y_p)\ddot{\theta}_1 \tag{24c}$$

$$\ddot{x}_p = \ddot{u}_1 + x\ddot{\varepsilon}_c - y_p(\ddot{v}_{,x} - \ddot{v}_1') - z_p(\ddot{w}_{,x} - \ddot{w}_1') \tag{25}$$

$$\ddot{\varepsilon}_c = \frac{\ddot{u}_2 - \ddot{u}_1}{L} + \frac{y_p}{L}(\ddot{v}_2' - \ddot{v}_1') + \frac{z_p}{L}(\ddot{w}_2' - \ddot{w}_1'). \tag{26}$$

Substituting Eqs. (11) and (20)–(26) into Eq. (17), and using $\int y\mathrm{d}A = \int z\mathrm{d}A = \int yz\mathrm{d}A = 0$, $\int \omega\mathrm{d}A = \int y\omega\mathrm{d}A = \int z\omega\mathrm{d}A = 0$, one may obtain

$$\mathbf{f}_a^d = AE\varepsilon_c\mathbf{G}_a \tag{27a}$$

$$\mathbf{f}_b^d = EI_z\int \mathbf{N}_b''v_{,xx}\mathrm{d}x + y_pAE\varepsilon_c\mathbf{B} \tag{27b}$$

$$\mathbf{f}_c^d = EI_y\int \mathbf{N}_c''w_{,xx}\mathrm{d}x + z_pAE\varepsilon_c\mathbf{C} \tag{27c}$$

$$\mathbf{f}_d^d = GJ\int \mathbf{N}_d'\theta_{1,x}\mathrm{d}x + EI_\omega\int \mathbf{N}_d''\theta_{1,xx}\mathrm{d}x \tag{27d}$$

$$\mathbf{B} = \{0, -1, 0, 1\}, \qquad \mathbf{C} = \{0, 1, 0, -1\}, \qquad \mathbf{G}_a = \{-1, 1\} \tag{28}$$

$$\begin{aligned}\mathbf{f}_a^I &= \rho A\int \mathbf{N}_a\mathbf{N}_a^t\mathrm{d}x\ddot{\mathbf{u}}_a + \rho Ay_p\int \mathbf{N}_a\mathbf{N}_e^t\mathrm{d}x\ddot{\mathbf{u}}_b \\ &\quad + \rho Az_p\int \mathbf{N}_a\mathbf{N}_f^t\mathrm{d}x\ddot{\mathbf{u}}_c\end{aligned} \tag{29a}$$

$$\begin{aligned}\mathbf{f}_b^I &= \rho A\int \mathbf{N}_b\ddot{v}\mathrm{d}x + \rho I_z\int \mathbf{N}_b'\ddot{v}'\mathrm{d}x \\ &\quad + \rho Ay_p\int \mathbf{N}_e\mathbf{N}_a^t\mathrm{d}x\ddot{\mathbf{u}}_a + \rho Ay_p^2\int \mathbf{N}_e\mathbf{N}_e^t\mathrm{d}x\ddot{\mathbf{u}}_b \\ &\quad + \rho Ay_pz_p\int \mathbf{N}_e\mathbf{N}_f^t\mathrm{d}x\ddot{\mathbf{u}}_c + \rho Az_p\int \mathbf{N}_b\ddot{\theta}_1\mathrm{d}x\end{aligned} \tag{29b}$$

$$\begin{aligned}\mathbf{f}_c^I &= \rho A\int \mathbf{N}_c\ddot{w}\mathrm{d}x + \rho I_y\int \mathbf{N}_c'\ddot{w}'\mathrm{d}x \\ &\quad + \rho Az_p\int \mathbf{N}_f\mathbf{N}_a^t\mathrm{d}x\ddot{\mathbf{u}}_a + \rho Az_p^2\int \mathbf{N}_f\mathbf{N}_f^t\mathrm{d}x\ddot{\mathbf{u}}_c \\ &\quad + \rho Ay_pz_p\int \mathbf{N}_f\mathbf{N}_e^t\mathrm{d}x\ddot{\mathbf{u}}_b - \rho Ay_p\int \mathbf{N}_c\ddot{\theta}_1\mathrm{d}x\end{aligned} \tag{29c}$$

$$\begin{aligned}\mathbf{f}_d^I &= \rho(I_y + I_z)\int \mathbf{N}_d\ddot{\theta}_1\mathrm{d}x + \rho I_\omega\int \mathbf{N}_d'\ddot{\theta}_{1,x}\mathrm{d}x \\ &\quad + \rho Az_p\int \mathbf{N}_d\ddot{v}\mathrm{d}x - \rho Ay_p\int \mathbf{N}_d\ddot{w}\mathrm{d}x \\ &\quad + \rho A(y_p^2 + z_p^2)\int \mathbf{N}_d\ddot{\theta}_1\mathrm{d}x\end{aligned} \tag{29d}$$

$$\ddot{\mathbf{u}}_a = \{\ddot{u}_1, \ddot{u}_2\}, \qquad \mathbf{N}_a = \left\{\frac{1-\xi}{2}, \frac{1+\xi}{2}\right\},$$

$$\mathbf{N}_e = -\mathbf{N}_f = \left\{0, \frac{1-\xi}{2}, 0, \frac{1+\xi}{2}\right\} \tag{30a}$$

$$I_y = \int z^2\mathrm{d}A, \qquad I_z = \int y^2\mathrm{d}A, \qquad I_\omega = \int \omega^2\mathrm{d}A \tag{30b}$$

$$J = \int\{[-(z - z_p) + \omega_{,y}]^2 + [(y - y_p) + \omega_{,z}]^2\}\mathrm{d}A \tag{30c}$$

in which the range of integration for the integral $\int(\ )\mathrm{d}x$ in Eqs. (27) and (29) is from 0 to L, A is the cross section area, $\mathbf{N}_k$ $(k = b, c, d)$ are given in Eq. (11). J in Eq. (27d), defined in Eq. (30c), is the torsional constant of the beam [27].

2.5. Element stiffness matrices and mass matrices

The element stiffness matrix and mass matrix may be obtained by differentiating the element nodal force with respect to nodal parameters and their time derivatives.

Using the direct stiffness method, the element tangent stiffness matrix may be assembled by the submatrices

$$\mathbf{k}_{ij} = \frac{\partial \mathbf{f}_i^d}{\partial \mathbf{u}_j} \tag{31}$$

where $\mathbf{f}_i^d$ $(i = a, b, c, d)$ are defined in Eq. (27) and $\mathbf{u}_j$ $(j = a, b, c, d)$ are defined in Eqs. (12) and (18). The explicit form of $\mathbf{k}_{ij}$ may be expressed as

$$\mathbf{k}_{aa} = \frac{AE}{L}\mathbf{G}_a\mathbf{G}_a^t, \qquad \mathbf{k}_{ab} = \underline{\frac{AE}{L}y_p\mathbf{G}_a\mathbf{B}^t}, \qquad \mathbf{k}_{ac} = \underline{\frac{AE}{L}z_p\mathbf{G}_a\mathbf{C}^t}, \qquad \mathbf{k}_{ad} = \mathbf{0}_{2\times4} \tag{32a}$$

$$\mathbf{k}_{bb} = EI_z\int \mathbf{N}_b''\mathbf{N}_b''^t\mathrm{d}x + \underline{\frac{AEy_p^2}{L}\mathbf{B}\mathbf{B}^t}, \qquad \mathbf{k}_{bc} = \underline{\frac{AEy_pz_p}{L}\mathbf{B}\mathbf{C}^t}, \qquad \mathbf{k}_{bd} = \mathbf{0}_{4\times4} \tag{32b}$$

$$\mathbf{k}_{cc} = EI_y\int \mathbf{N}_c''\mathbf{N}_c''^t\mathrm{d}x + \underline{\frac{AEz_p^2}{L}\mathbf{C}\mathbf{C}^t}, \qquad \mathbf{k}_{cd} = \mathbf{0}_{4\times4} \tag{32c}$$

$$\mathbf{k}_{dd} = GJ\int \mathbf{N}_d'\mathbf{N}_d'^t\mathrm{d}x + EI_\omega\int \mathbf{N}_d''\mathbf{N}_d''^t\mathrm{d}x. \tag{32d}$$

Using the direct stiffness method, the element mass matrix may be assembled by the submatrices

$$\mathbf{m}_{ij} = \frac{\partial \mathbf{f}_i^I}{\partial \ddot{\mathbf{u}}_j} \tag{33}$$

where and $\mathbf{f}_i^I$ $(i = a, b, c, d)$ are defined in Eq. (29). The explicit form of $\mathbf{m}_{ij}$ may be expressed as

$$\mathbf{m}_{aa} = \rho A\int \mathbf{N}_a\mathbf{N}_a^t\mathrm{d}x, \qquad \mathbf{m}_{ab} = \underline{\rho Ay_p\int \mathbf{N}_a\mathbf{N}_e^t\mathrm{d}x}, \qquad \mathbf{m}_{ac} = \underline{\rho Az_p\int \mathbf{N}_a\mathbf{N}_f^t\mathrm{d}x}, \qquad \mathbf{m}_{ad} = \mathbf{0}_{2\times4} \tag{34a}$$

$$\mathbf{m}_{bb} = \rho A\int \mathbf{N}_b\mathbf{N}_b^t\mathrm{d}x + \rho I_z\int \mathbf{N}_b'\mathbf{N}_b'^t\mathrm{d}x + \underline{\rho Ay_p^2\int \mathbf{N}_e\mathbf{N}_e^t\mathrm{d}x}, \qquad \mathbf{m}_{bc} = \underline{\rho Ay_pz_p\int \mathbf{N}_e\mathbf{N}_f^t\mathrm{d}x}, \qquad \mathbf{m}_{bd} = \rho Az_p\int \mathbf{N}_b\mathbf{N}_d^t\mathrm{d}x \tag{34b}$$

$$\mathbf{m}_{cc} = \rho A \int \mathbf{N}_c \mathbf{N}_c^t \mathrm{d}x + \rho I_y \int \mathbf{N}_c' \mathbf{N}_c'^t \mathrm{d}x + \rho A z_p^2 \int \mathbf{N}_f \mathbf{N}_f^t \mathrm{d}x, \tag{34c}$$

$$\mathbf{m}_{cd} = -\rho A y_p \int \mathbf{N}_c \mathbf{N}_d^t \mathrm{d}x$$

$$\mathbf{m}_{dd} = \rho (I_y + I_z) \int \mathbf{N}_d \mathbf{N}_d^t \mathrm{d}x + \rho I_\omega \int \mathbf{N}_d' \mathbf{N}_d'^t \mathrm{d}x + \rho A (y_p^2 + z_p^2) \int \mathbf{N}_d \mathbf{N}_d^t \mathrm{d}x. \tag{34d}$$

2.6. The relation between element matrices corresponding to different element nodal degrees of freedom

Let $\delta \mathbf{u}_j^Q = \{\delta u_j^Q, \delta v_j^Q, \delta w_j^Q\}$ and $\delta \mathbf{u}_j^P = \{\delta u_j, \delta v_j, \delta w_j\}$ $(j = 1, 2)$ denote virtual displacements of an arbitrary point Q and shear center P of the cross sections corresponding to element nodes j, respectively. In this study, $Q = C$ and $Q = R$ are considered, where C and R denote centroid and a point rather than a centroid and shear center, respectively. Making use of the assumption that the cross section of the beam element does not deform in its own plane, the relation between $\delta \mathbf{u}_j^Q$ $(Q = C, R)$ and $\delta \mathbf{u}_j^P$ may be expressed by

$$\delta \mathbf{u}_j^P = \delta \mathbf{u}_j^Q + \delta \boldsymbol{\varphi}_j \times \mathbf{r}_{QP} \tag{35}$$

$$\delta u_j = \delta u_j^Q - y_{qp} \delta \varphi_{3j} + z_{qp} \delta \varphi_{2j} \tag{36a}$$

$$\delta v_j = \delta v_j^Q - z_{qp} \delta \varphi_{1j} \tag{36b}$$

$$\delta w_j = \delta w_j^Q + y_{qp} \delta \varphi_{1j} \tag{36c}$$

where $\mathbf{r}_{QP} = \{0, y_{qp}, z_{qp}\} = \{0, y_p - y_q, z_p - z_q\}$, y_p and z_p, and y_q and z_q are the x_2^S and x_3^S coordinates of point P and Q referred to the element cross section coordinates, respectively, $\delta \varphi_{ij}$ $(i = 1, 2, 3,\ j = 1, 2)$ are virtual rotations about x_i axes at nodes j.

From Eqs. (35) and (36), one may obtain

$$\delta \mathbf{q}_P = \mathbf{T}_{PQM} \delta \mathbf{q}_{QM} \tag{37}$$

$$\delta \mathbf{q}_P = \mathbf{T}_{PQ} \delta \mathbf{q}_Q \tag{38}$$

$$\delta \mathbf{q}_P = \{\delta \mathbf{u}_a, \delta \mathbf{u}_b, \delta \mathbf{u}_c, \delta \mathbf{u}_d\} \tag{39}$$

$$\delta \mathbf{q}_{QM} = \{\delta \mathbf{u}_a^Q, \delta \mathbf{u}_b, \delta \mathbf{u}_c, \delta \mathbf{u}_d\} \tag{40}$$

$$\delta \mathbf{q}_Q = \{\delta \mathbf{u}_a^Q, \delta \mathbf{u}_b^Q, \delta \mathbf{u}_c^Q, \delta \mathbf{u}_d\} \tag{41}$$

$$\mathbf{T}_{PQM} = \begin{bmatrix} \mathbf{I}_{2\times2} & \mathbf{T}_1 & \mathbf{T}_2 & \mathbf{0}_{2\times4} \\ \mathbf{0}_{4\times2} & \mathbf{I}_{4\times4} & \mathbf{0}_{4\times4} & \mathbf{0}_{4\times4} \\ \mathbf{0}_{4\times2} & \mathbf{0}_{4\times4} & \mathbf{I}_{4\times4} & \mathbf{0}_{4\times4} \\ \mathbf{0}_{4\times2} & \mathbf{0}_{4\times4} & \mathbf{0}_{4\times4} & \mathbf{I}_{4\times4} \end{bmatrix}, \tag{42a}$$

$$\mathbf{T}_{PQ} = \begin{bmatrix} \mathbf{I}_{2\times2} & \mathbf{T}_1 & \mathbf{T}_2 & \mathbf{0}_{2\times4} \\ \mathbf{0}_{4\times2} & \mathbf{I}_{4\times4} & \mathbf{0}_{4\times4} & \mathbf{T}_3 \\ \mathbf{0}_{4\times2} & \mathbf{0}_{4\times4} & \mathbf{I}_{4\times4} & \mathbf{T}_4 \\ \mathbf{0}_{4\times2} & \mathbf{0}_{4\times4} & \mathbf{0}_{4\times4} & \mathbf{I}_{4\times4} \end{bmatrix} \tag{42b}$$

where

$$\delta \mathbf{u}_a^Q = \{\delta u_1^Q, \delta u_2^Q\}, \tag{43a}$$

$$\delta \mathbf{u}_b^Q = \{\delta v_1^Q, \delta \varphi_{31}, \delta v_2^Q, \delta \varphi_{32}\}, \tag{43b}$$

$$\delta \mathbf{u}_c^Q = \{\delta w_1^Q, \delta \varphi_{21}, \delta w_2^Q, \delta \varphi_{22}\} \tag{43c}$$

$$\mathbf{T}_1 = \begin{bmatrix} 0 & -y_{qp} & 0 & 0 \\ 0 & 0 & 0 & -y_{qp} \end{bmatrix}, \tag{44a}$$

$$\mathbf{T}_2 = \begin{bmatrix} 0 & z_{pq} & 0 & 0 \\ 0 & 0 & 0 & z_{pq} \end{bmatrix}, \tag{44b}$$

$$\mathbf{T}_3 = \begin{bmatrix} -z_{qp} & 0 & 0 & 0 \\ 0 & 0 & 0 & 0 \\ 0 & 0 & -z_{qp} & 0 \\ 0 & 0 & 0 & 0 \end{bmatrix}, \tag{44c}$$

$$\mathbf{T}_4 = \begin{bmatrix} y_{qp} & 0 & 0 & 0 \\ 0 & 0 & 0 & 0 \\ 0 & 0 & y_{qp} & 0 \\ 0 & 0 & 0 & 0 \end{bmatrix}. \tag{44d}$$

Let $\mathbf{k}_{QM}$, $\mathbf{k}_Q$ and $\mathbf{k}_P$ denote the element stiffness matrices corresponding to $\delta \mathbf{q}_{QM}$, $\delta \mathbf{q}_Q$ and $\delta \mathbf{q}_P$, respectively. The relation between $\mathbf{k}_{QM}$ and $\mathbf{k}_P$, and the relation between $\mathbf{k}_Q$ and $\mathbf{k}_P$ may be expressed by

$$\mathbf{k}_{QM} = \mathbf{T}_{PQM}^t \mathbf{k}_P \mathbf{T}_{PQM} \tag{45a}$$

$$\mathbf{k}_Q = \mathbf{T}_{PQ}^t \mathbf{k}_P \mathbf{T}_{PQ} \tag{45b}$$

$$\mathbf{k}_{QM} = \begin{bmatrix} \mathbf{k}_{aa}^{QM} & \mathbf{k}_{ab}^{QM} & \mathbf{k}_{ac}^{QM} & \mathbf{k}_{ad}^{QM} \\ & \mathbf{k}_{bb}^{QM} & \mathbf{k}_{bc}^{QM} & \mathbf{k}_{bd}^{QM} \\ & & \mathbf{k}_{cc}^{QM} & \mathbf{k}_{cd}^{QM} \\ \text{sym.} & & & \mathbf{k}_{dd}^{QM} \end{bmatrix}, \tag{45c}$$

$$\mathbf{k}_Q = \begin{bmatrix} \mathbf{k}_{aa}^{Q} & \mathbf{k}_{ab}^{Q} & \mathbf{k}_{ac}^{Q} & \mathbf{k}_{ad}^{Q} \\ & \mathbf{k}_{bb}^{Q} & \mathbf{k}_{bc}^{Q} & \mathbf{k}_{bd}^{Q} \\ & & \mathbf{k}_{cc}^{Q} & \mathbf{k}_{cd}^{Q} \\ \text{sym.} & & & \mathbf{k}_{dd}^{Q} \end{bmatrix} \tag{45d}$$

$$\mathbf{k}_P = \begin{bmatrix} \mathbf{k}_{aa} & \mathbf{k}_{ab} & \mathbf{k}_{ac} & \mathbf{k}_{ad} \\ & \mathbf{k}_{bb} & \mathbf{k}_{bc} & \mathbf{k}_{bd} \\ & & \mathbf{k}_{cc} & \mathbf{k}_{cd} \\ \text{sym.} & & & \mathbf{k}_{dd} \end{bmatrix} \tag{45e}$$

where $\mathbf{k}_{ij}$ $(i = a, b, c, d,\ j = a, b, c, d)$ are defined in Eq. (32).

Let $\mathbf{m}_{QM}$, $\mathbf{m}_Q$ and $\mathbf{m}_P$ denote the element stiffness matrices corresponding to $\delta \mathbf{q}_{QM}$, $\delta \mathbf{q}_Q$ and $\delta \mathbf{q}_P$, respectively. The relation between $\mathbf{m}_{QM}$ and $\mathbf{m}_P$, and the relation between $\mathbf{m}_Q$ and $\mathbf{m}_P$ may be expressed by

$$\mathbf{m}_{QM} = \mathbf{T}_{PQM}^t \mathbf{m}_P \mathbf{T}_{PQM} \tag{46a}$$

$$\mathbf{m}_Q = \mathbf{T}_{PQ}^t \mathbf{m}_P \mathbf{T}_{PQ} \tag{46b}$$

$$\mathbf{m}_{QM} = \begin{bmatrix} \mathbf{m}_{aa}^{QM} & \mathbf{m}_{ab}^{QM} & \mathbf{m}_{ac}^{QM} & \mathbf{m}_{ad}^{QM} \\ & \mathbf{m}_{bb}^{QM} & \mathbf{m}_{bc}^{QM} & \mathbf{m}_{bd}^{QM} \\ & & \mathbf{m}_{cc}^{QM} & \mathbf{m}_{cd}^{QM} \\ \text{sym.} & & & \mathbf{m}_{dd}^{QM} \end{bmatrix}, \tag{46c}$$

$$\mathbf{m}_{Q} = \begin{bmatrix} \mathbf{m}_{aa}^{Q} & \mathbf{m}_{ab}^{Q} & \mathbf{m}_{ac}^{Q} & \mathbf{m}_{ad}^{Q} \\ & \mathbf{m}_{bb}^{Q} & \mathbf{m}_{bc}^{Q} & \mathbf{m}_{bd}^{Q} \\ & & \mathbf{m}_{cc}^{Q} & \mathbf{m}_{cd}^{Q} \\ \text{sym.} & & & \mathbf{m}_{dd}^{Q} \end{bmatrix} \tag{46d}$$

$$\mathbf{m}_{P} = \begin{bmatrix} \mathbf{m}_{aa} & \mathbf{m}_{ab} & \mathbf{m}_{ac} & \mathbf{m}_{ad} \\ & \mathbf{m}_{bb} & \mathbf{m}_{bc} & \mathbf{m}_{bd} \\ & & \mathbf{m}_{cc} & \mathbf{m}_{cd} \\ \text{sym.} & & & \mathbf{m}_{dd} \end{bmatrix} \tag{46e}$$

where $\mathbf{m}_{ij}$ $(i = a, b, c, d, j = a, b, c, d)$ are defined in Eq. (34).

If $Q = C$, then the explicit form of $\mathbf{k}_{ij}^{CM}$ and $\mathbf{m}_{ij}^{CM}$ $(i = a, b, c, d, j = a, b, c, d)$ in Eqs. (45c) and (46c) can be obtained by removing the underlined terms from $\mathbf{k}_{ij}$ and $\mathbf{m}_{ij}$ in Eqs. (32) and (34).

If $Q = C$, the explicit form of $\mathbf{k}_{ij}^{C}$ and $\mathbf{m}_{ij}^{C}$ $(i = a, b, c, d, j = a, b, c, d)$ in Eqs. (45d) and (46d) may be given by

$$\mathbf{k}_{aa}^{C} = \mathbf{k}_{aa}, \quad \mathbf{k}_{ab}^{C} = \mathbf{0}_{2\times4}, \quad \mathbf{k}_{ac}^{C} = \mathbf{0}_{2\times4}, \quad \mathbf{k}_{ad}^{C} = \mathbf{0}_{2\times4} \tag{47a}$$

$$\mathbf{k}_{bb}^{C} = \mathbf{k}_{bb}^{CM}, \quad \mathbf{k}_{bc}^{C} = \mathbf{0}_{4\times4}, \quad \mathbf{k}_{bd}^{C} = \mathbf{k}_{bb}\mathbf{T}_3 + \mathbf{T}_1^t\mathbf{k}_{ab}\mathbf{T}_3 \tag{47b}$$

$$\mathbf{k}_{cc}^{C} = \mathbf{k}_{cc}^{CM}, \quad \mathbf{k}_{cd}^{C} = \mathbf{k}_{cc}\mathbf{T}_4 + \mathbf{T}_2^t\mathbf{k}_{ac}\mathbf{T}_4 \tag{47c}$$

$$\mathbf{k}_{dd}^{C} = \mathbf{k}_{dd} + \mathbf{T}_4^t\mathbf{k}_{cb}\mathbf{T}_3 + \mathbf{T}_3^t\mathbf{k}_{bb}\mathbf{T}_3 + \mathbf{T}_4^t\mathbf{k}_{cc}\mathbf{T}_4 + \mathbf{T}_3^t\mathbf{k}_{bc}\mathbf{T}_4 \tag{47d}$$

$$\mathbf{m}_{aa}^{C} = \mathbf{m}_{aa}^{CM}, \quad \mathbf{m}_{ab}^{C} = \mathbf{0}_{2\times4}, \quad \mathbf{m}_{ac}^{C} = \mathbf{0}_{2\times4}, \quad \mathbf{m}_{ad}^{C} = \mathbf{0}_{2\times4} \tag{48a}$$

$$\mathbf{m}_{bb}^{C} = \mathbf{m}_{bb}^{CM}, \quad \mathbf{m}_{bc}^{C} = \mathbf{0}_{4\times4}, \quad \mathbf{m}_{bd}^{C} = \mathbf{m}_{bd} + \mathbf{m}_{bb}\mathbf{T}_3 + \mathbf{T}_1^t\mathbf{m}_{ab}\mathbf{T}_3 \tag{48b}$$

$$\mathbf{m}_{cc}^{C} = \mathbf{m}_{cc}^{CM}, \quad \mathbf{m}_{cd}^{C} = \mathbf{m}_{cd} + \mathbf{m}_{cc}\mathbf{T}_4 + \mathbf{T}_2^t\mathbf{m}_{ac}\mathbf{T}_4 \tag{48c}$$

$$\mathbf{m}_{dd}^{C} = \mathbf{m}_{dd} + \mathbf{T}_4^t\mathbf{m}_{cd} + \mathbf{m}_{cd}^t\mathbf{T}_4 + \mathbf{T}_3^t\mathbf{m}_{bd} + \mathbf{m}_{bd}^t\mathbf{T}_3 + \mathbf{T}_3^t\mathbf{m}_{bc}\mathbf{T}_4 + \mathbf{T}_4^t\mathbf{m}_{bc}^t\mathbf{T}_3 + \mathbf{T}_3^t\mathbf{m}_{bb}\mathbf{T}_3 + \mathbf{T}_4^t\mathbf{m}_{cc}\mathbf{T}_4. \tag{48d}$$

It can be seen from Eqs. (32), (34), (47a) and (48a) that if the axial displacement is restrained at the centroid of the cross section, the axial vibration is uncoupled from bending vibrations and torsional vibration as reported in the literature. However, if the axial displacement of the pin end is restrained at a point Q of the cross section ($y_q \neq 0, z_q \neq 0$) for a monosymmetric beam or an asymmetric beam, the axial vibration, two bending vibrations, and torsional vibration are all coupled. If the axial and lateral displacements are all restrained at the centroid of the cross section, the axial vibration is still uncoupled from bending vibrations and torsional vibration. However, the coupled bending and torsional vibrations corresponding to $\delta\mathbf{q}_{CM}$, $\delta\mathbf{q}_{C}$ are different if the axial rotation is not restrained.

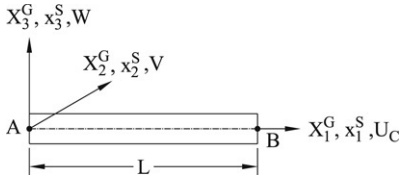

Fig. 2. Coordinate systems and notation for all examples.

2.7. Frequency equations for linear free vibration

The natural frequencies and vibration modes of the discrete structural system may be determined from the generalized eigenvalue problem expressed by

$$\mathbf{KQ} = \omega^2\mathbf{MQ} \tag{49}$$

where ω, $\mathbf{M}$, $\mathbf{K}$ and $\mathbf{Q}$ are the natural frequency, structural mass matrix, stiffness matrix, and vibration mode, respectively. Here, the natural frequencies and vibrations modes are solved by using the subspace iteration method [33].

3. Numerical studies

For all examples studied here, the global coordinates as shown in Fig. 2 are chosen to coincide with the element cross section coordinates. For all examples, the present results are obtained using 20 elements. The vibration modes plotted are U_C, axial displacement of the centroid axis, V and W, lateral displacements of the shear center axis in the X_2^G and X_3^G directions, respectively, and ϕ_1, the twist angle about the shear center axis.

Different boundary conditions for end sections A and B of the beam given in Fig. 2 are considered here. For convenience, in this study, $BCIX$, $I = 1-5, X = P, CM, RM, C, R$ are used to denote boundary conditions I corresponding to nodal degrees of freedom $\mathbf{q}_X$. P, C, and R express that nodal degrees of freedom corresponding to the axial and the lateral displacements are all defined at the shear center P, centroid C and point R of the end section, respectively. CM and RM express that nodal degrees of freedom corresponding to the axial displacement are defined at centroid C and point R of the end section, respectively, and the lateral displacements are all defined at the shear center P of the end section. The boundaries considered here are given by

$BC1$: $u_A^X = 0, v_A^X = v_B^X = 0, w_A^X = w_B^X = 0, \theta_{1A} = \theta_{1B} = 0$

$BC2$: $u_A^X = 0, v_A^X = 0, v_A'^X = 0, w_A^X = 0, w_A'^X = 0, \theta_{1A} = 0, \beta_A = 0$

$BC3$: $u_A^X = u_B^X = 0, v_A^X = v_B^X = 0, v_A'^X = v_B'^X = 0, w_A^X = w_B^X = 0, w_A'^X = w_B'^X = 0, \theta_{1A} = \theta_{1B} = 0, \beta_A = \beta_B = 0$

$BC4$: $u_A^X = 0, v_A^X = v_B^X = 0, v_A'^X = 0, w_A^X = w_B^X = 0, w_A'^X = 0, \theta_{1A} = 0, \beta_A = 0$

Table 1
Natural frequencies (rad/s) of example 1 (monosymmetric channel section)

Mode	$BC1P$	$BC1CM(C)$	$BC1CM$ [19]	$BC1RM(R)$	$BC2X$	$BC2CM$ [19]	$BC3X$	$BC3CM$ [19]
1	421.59 (W,T)	421.59 (W,T)	421.73	421.57	159.38 (W,T)	159.40	938.20 (W,T)	938.71
2	587.73 (A,V)	592.83 (V)	N/A	587.70	211.31 (V)	N/A	1343.52 (V)	N/A
3	1653.48 (W,T)	1653.48 (W,T)	1656.69	1652.91	616.68 (W,T)	619.21	2573.86 (W,T)	2579.75
4	1717.33 (W,T)	1717.33 (W,T)	1732.59	1688.39	932.51 (W,T)	934.00	3690.20 (V)	N/A
5	2270.23 (A,V)	2363.83 (V)	N/A	2273.52	1320.33 (V)	N/A	3880.90 (W,T)	3924.04
6	3698.25 (W,T)	3698.25 (W,T)	3714.81	3695.20	2575.91 (W,T)	2585.97	5025.75 (W,T)	5050.68
7	4473.19 (A,V)	5291.02 (V)	N/A	4337.38	3679.45 (V)	N/A	7194.27 (V)	N/A
8	6288.05 (A,V)	6445.14 (A)	N/A	5896.49	3757.01 (W,T)	3866.61	8272.94 (W,T)	8344.01
9	6544.06 (W,T)	6544.06 (W,T)	6596.09	6545.51	5018.13 (W,T)	N/A	10 387.2 (W,T)	N/A
10	6687.65 (W,T)	6687.65 (W,T)	N/A	7094.14	6445.14 (A)	N/A	11 803.9 (V)	N/A
Mode	$BC4P$(QM)	$BC4C$	$BC4R$	$BC5P$	$BC5CM$	$BC5RM$	$BC5C$	$BC5R$
1	163.61 (W,T)	408.32 (W,T)	178.45 (V,W,T)	163.61 (W,T)	163.61 (W,T)	163.62	408.32 (W,T)	214.67
2	925.95 (V)	823.00 (W,T)	768.58 (V,W,T)	932.01 (W,T)	925.95 (V)	931.96	823.00 (W,T)	782.78
3	932.01 (W,T)	925.95 (V)	1118.52 (V,W,T)	1082.89 (A,V)	932.01 (W,T)	1064.72	925.95 (V)	1268.26
4	2554.59 (W,T)	2176.52 (W,T)	2367.26 (V,W,T)	2554.59 (W,T)	2554.59 (W,T)	2565.70	2176.52 (W,T)	2369.86
5	2700.77 (W,T)	2990.64 (V)	2680.95 (V,W,T)	2700.77 (W,T)	2700.77 (W,T)	2749.00	2990.64 (V)	2736.22
6	2990.64 (V)	3364.10 (W,T)	3236.91 (V,W,T)	3144.22 (A,V)	2990.64 (V)	3163.62	3364.10 (W,T)	3431.85
7	5015.73 (W,T)	4677.57 (W,T)	4799.19 (V,W,T)	5015.73 (W,T)	5015.73 (W,T)	5016.39	4677.57 (W,T)	4800.71
8	6206.27 (V)	6206.27 (V)	6445.14 (A)	6225.49 (A,V)	6206.27 (V)	6225.34	6206.27 (V)	6453.34
9	6445.14 (A)	6445.14 (A)	6454.25 (V,W,T)	8218.19 (W,T)	8218.19 (W,T)	8166.81	7541.26 (W,T)	8027.73
10	8218.19 (W,T)	7541.26 (W,T)	8039.06 (V,W,T)	8475.59 (W,T)	8475.59 (W,T)	8357.95	9555.59 (W,T)	8270.84

$X = P, CM, RM, C, R$.

$BC5$: $u_A^X = u_B^X = 0$, $v_A^X = v_B^X = 0$, $v_A'^X = 0$, $w_A^X = w_B^X = 0$, $w_A'^X = 0$, $\theta_{1A} = 0$, $\beta_A = 0$

where $j = A, B$, β_j denote the twist rate of the shear center axis at end sections j. Due to the assumption that the out-of-plane warping of the cross section is the product of the twist rate of the beam element and the Saint Venant warping function, $\beta_j = 0$ denote warping restrained at end sections j. $BC1$ refers to both ends hinged. However, the axial displacement is only restrained at end A. Torsion is restrained but warping free at both supports. $BC2$ refers to one end fixed and one end free. The axial displacement, lateral displacements, torsion and warping are all restrained at one end and all free at the other end. $BC3$ refers to both ends fixed. The axial displacement, lateral displacements, torsion and warping are all restrained at both supports. $BC4$ refers to one end fixed and one end hinged. However, only the lateral displacements are restrained at the hinged end. The axial displacement, torsion and warping are free at the hinged end. $BC5$ refers to one end fixed and one end hinged. However, the axial displacement and the lateral displacements are restrained at the hinged end. The torsion and warping are free at the hinged end. Due to the assumption that the cross section of the beam element does not deform in its own plane, the fixed end and free end corresponding to different nodal degrees of freedom $\mathbf{q}_X$ are equivalent. Thus, the boundary conditions $BC2X$ are equivalent and $BC3X$ are equivalent for $X = P, RM, CM, C, R$. From Eq. (36), it can be seen that boundary conditions $BC1CM$ and $BC1C$ are equivalent, $BC1RM$ and $BC1R$ are equivalent, and $BC4P$, $BC4CM$ and $BC4RM$ are equivalent.

3.1. Example 1. Monosymmetric channel cross section

The example considered here is a uniform beam with monosymmetric channel cross section as shown in Fig. 3. This example was studied in [19] for boundary conditions $BCICM$ $(I = 1, 2, 3)$. The geometry and material properties are given in Fig. 3. The section constants are as follows:

$$A = 2.669 \times 10^{-4} m^2, \qquad I_y = 4.5 \times 10^{-7} m^4,$$
$$I_z = 9.396 \times 10^{-8} m^4, \qquad J = 1.4 \times 10^{-10} m^4,$$
$$I_\omega = 1.636 \times 10^{-10} m^6.$$

The lowest 10 natural frequencies of the present study together with those given in [19] are shown in Table 1. It can be seen that the agreement between the natural frequencies of the present study and those given in [19] is very good. In Table 1, (A) and (V) denote that the natural frequency corresponds to uncoupled axial vibration and bending vibration in the X_2^G direction, respectively; (A, V) denotes that the natural frequency corresponds to coupled axial vibration and bending vibration in the X_2^G direction; (W, T) denotes that the natural frequency corresponds to coupled torsional vibration and bending vibration in the X_3^G direction, (V, W, T) denotes that the natural frequency corresponds to the coupled bending vibration in the X_2^G and X_3^G directions and torsional vibration. It can be seen that for boundary conditions $BC1CM(C)$, $BC2X$, $BC3X$, $BC4P(RM)$, $BC4C$ and $BC5C$, the vibrations are a coupled (W, T) vibration, uncoupled (A) vibration and uncoupled (V) vibration; for boundary conditions $BC1P$ and $BC5P$, the vibrations are a coupled (A, V) vibration and a coupled (W, T) vibration; for boundary condition $BC4R$, the vibrations are a triply coupled (V, W, T) vibration and an uncoupled (A) vibration; for

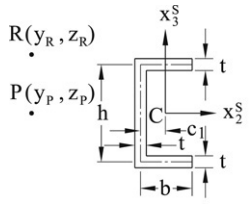

b = 57.375 mm	L = 1.28 m
h = 98.75 mm	E = 216.4 GPa
t = 1.25 mm	G = 80.1 GPa
c_1 = 15.42 mm	m = 2.095 kg/m
y_P = −37.71 mm	
z_P = 0	
y_R = −37.71 mm	
z_R = 37.71 mm	

Fig. 3. Monosymmetric channel cross section for example 1.

boundary conditions $BC1RM(R)$, $BC5RM$, $BC5R$, the axial vibration, two bending vibrations, and torsional vibration are all coupled (quadruply coupled vibration). The natural frequencies corresponding to the (W, T) vibration are identical for boundary conditions $BC1P$ and $BC1CM(C)$. The vibration modes corresponding to the lowest 10 natural frequencies for boundary condition $BC1RM$, $BC4R$, $BC5RM$ and $BC5R$ are shown in Figs. 4–7.

3.2. Example 2. Monosymmetric T cross section

The example considered here is a uniform beam with a monosymmetric T cross section as shown in Fig. 8. This example was studied in [21] for boundary condition $BC1CM$. The geometry and material properties are given in Fig. 4. The section constants are as follows:

$$A = 1925.2 \times 10^{-6} m^2, \qquad I_y = 7.6839 \times 10^{-6} m^4,$$
$$I_z = 7.11143 \times 10^{-7} m^4, \qquad J = 3.17103 \times 10^{-8} m^4,$$
$$I_\omega = 3.86899 \times 10^{-11} m^6.$$

The lowest 10 natural frequencies of the present study are shown in Table 2. The first uncoupled axial natural frequency for the boundary condition $BC1CM$ may be given by $\pi/L\sqrt{E/\rho} = 8150.45$ rad/s, which is much larger than the lowest 10 natural frequencies for the boundary condition $BC1CM$. The first natural frequency given in [21] for boundary condition $BC1CM$ is 191.49 rad/s. In Table 2, (W) expresses that the natural frequency corresponds to the uncoupled axial vibration and the bending vibration in the X_2^G direction, respectively; (A, W) expresses that the natural frequency corresponds to the coupled axial vibration and the bending vibration in the X_2^G direction; (V, T) expresses that the natural frequency corresponds to the coupled torsional vibration and the bending vibration in the X_3^G direction, (V, W, T) denotes that the natural frequency corresponds to the coupled bending vibration in the X_2^G and X_3^G directions and torsional vibration. It can be seen that for the boundary conditions $BC1CM(C)$, $BC2X$, $BC3X$, $BC4P(RM)$, $BC4C$ and $BC5C$, the vibrations are a coupled (V, T) vibration, and

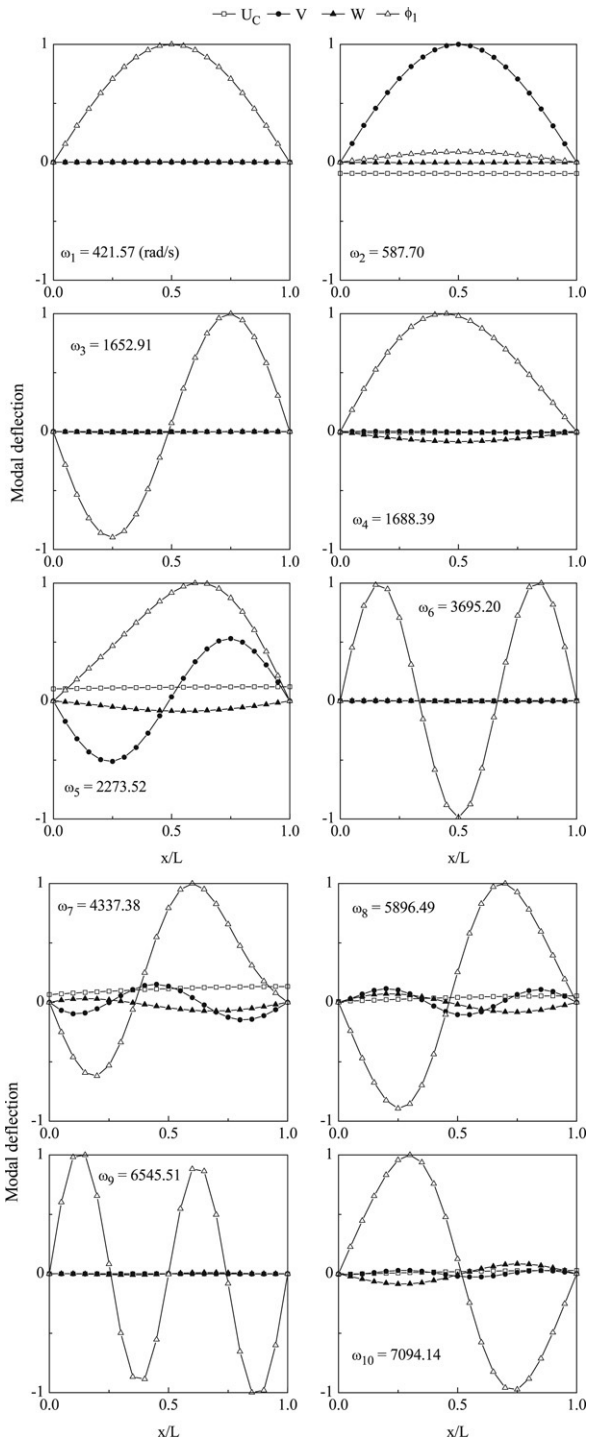

Fig. 4. The first 10 vibration mode shapes for example 1 ($BC1RM$).

an uncoupled (W) vibration; for boundary conditions $BC1P$ and $BC5P$, the vibrations are a coupled (A, W) vibration and a coupled (V, T) vibration; for boundary condition $BC4R$, the vibrations are a triply coupled (V, W, T) vibration; for boundary conditions $BC1RM(R)$, $BC5RM$, $BC5R$, the axial vibration, two bending vibrations and torsional vibration are all coupled (quadruply coupled vibration). The natural frequencies corresponding to (W, T) vibration are identical for boundary conditions $BC1P$ and $BC1CM(C)$.

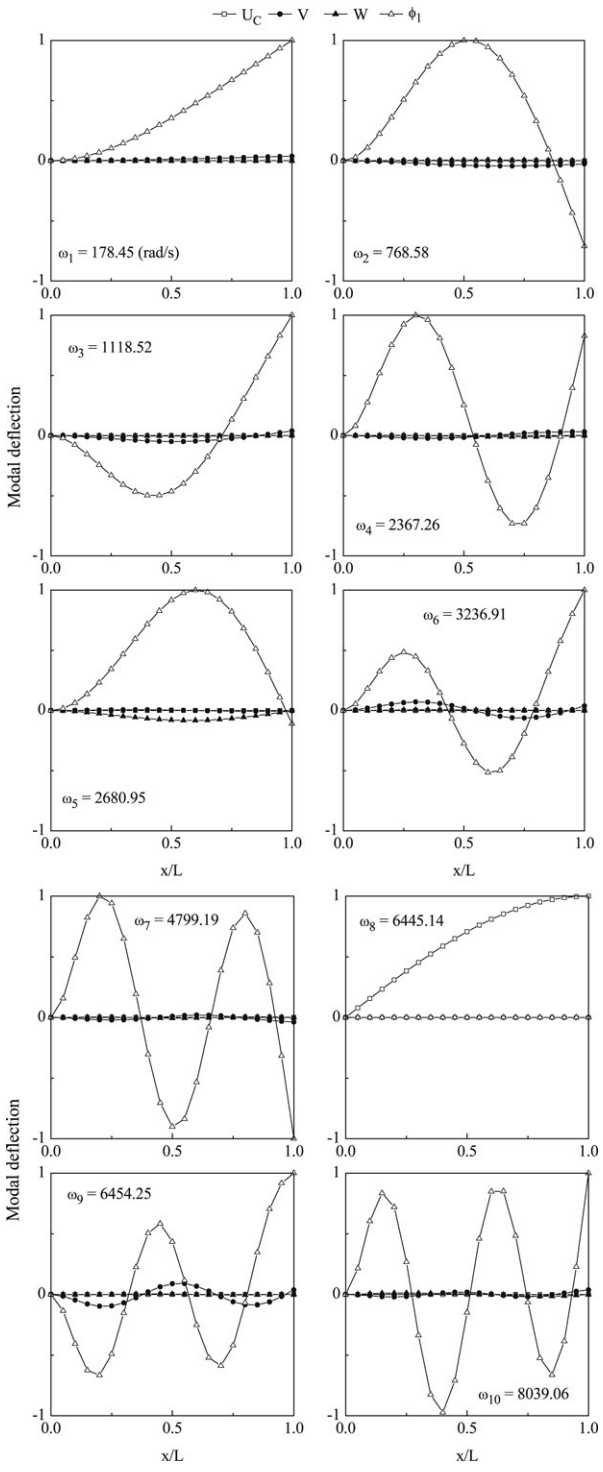

Fig. 5. The first 10 vibration mode shapes for example 1 ($BC4R$).

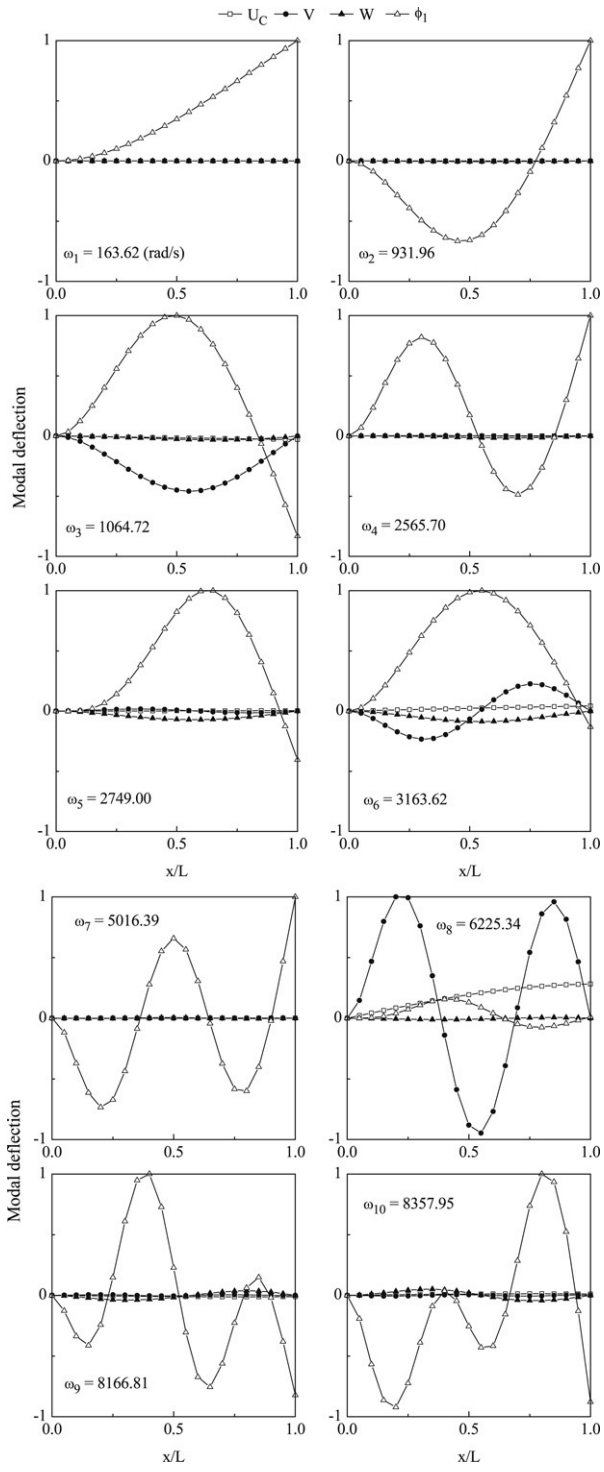

Fig. 6. The first 10 vibration mode shapes for example 1 ($BC5RM$).

3.3. Example 3. Asymmetric cross section A

The example considered here is a uniform beam with an asymmetric cross section as shown in Fig. 9. This example was studied in [22] for boundary conditions $BC1CM$. The geometry and material properties are given in Fig. 9. The section constants are as follows: $A = 3.4 \times 10^{-2}m^2$, $I_y = 5.81146 \times 10^{-4}m^4$, $I_z = 1.75303 \times 10^{-3}m^4$, $J = 4.53333 \times 10^{-6}m^4$, $I_\omega = 1.28016 \times 10^{-4}m^6$.

The lowest 13 natural frequencies of the present study together with those given in [22] are shown in Table 3. In Table 3, (A) denotes that the natural frequency corresponds to uncoupled axial vibration. It can be seen that the agreement between the natural frequencies of the present study and those given in [22] is very good. For boundary conditions $BC1P$ and $BC5P$, the axial displacements are restrained at the shear center P ($y_p \neq 0$, $z_p \neq 0$) of the cross section of pin ends A and B, respectively. Thus, as mentioned in the previous

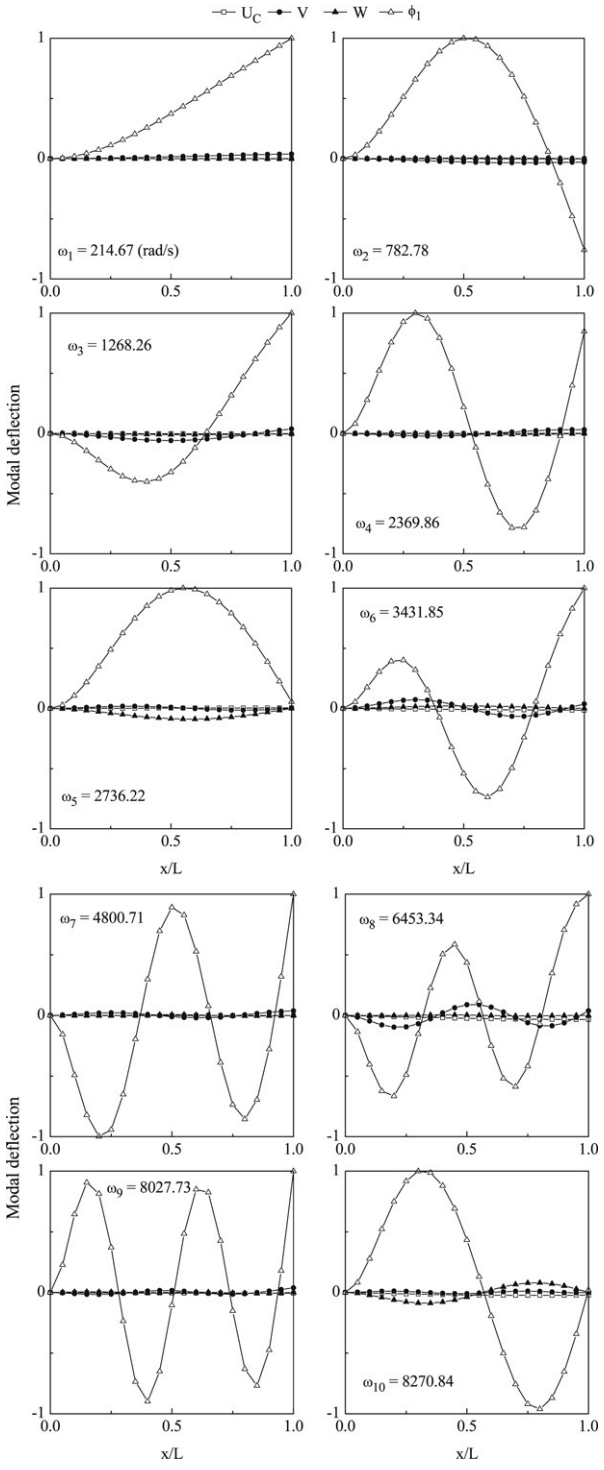

Fig. 7. The first 10 vibration mode shapes for example 1 ($BC5R$).

section, for boundary conditions $BC1P$ and $BC5P$, the axial vibration, two bending vibrations and torsional vibration are all coupled (quadruply coupled vibration). For the rest of the boundary conditions, only two bending vibrations and the torsional vibration are coupled (triply coupled vibration). The vibration modes corresponding to the lowest 10 natural frequencies for boundary conditions $BC1P$, $BC1CM$, $BC4P$, $BC4C$, and $BC5P$ are shown in Figs. 10–14. It can be seen

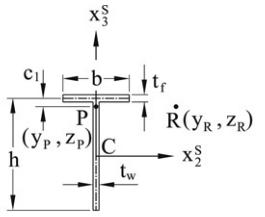

h = 192 mm L = 2 m
b = 100 mm E = 210 GPa
t_f = 8.5 mm G = 80.77 GPa
t_w = 5.6 mm ρ = 7800 kg/m³
c_1 = 0.379313 mm
y_P = 0
z_P = 53.88 mm
y_R = 53.88 mm
z_R = 53.88 mm

Fig. 8. Monosymmetric T cross section for example 2.

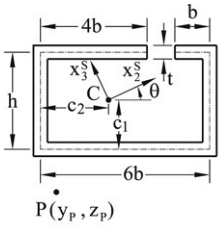

θ = −0.04070 rad L = 10 m
b = 0.1 m E = 210 GPa
h = 0.3 m G = 80.7 GPa
t = 0.02 m ρ = 8.002 kN·s²/m⁴
c_1 = 0.14118 m
c_2 = 0.29118 m
y_P = −0.23526 m
z_P = −0.31147 m

Fig. 9. Asymmetric cross section A for example 3.

from Figs. 10 and 11 that the coupling characteristics of free vibration for the boundary conditions $BC1P$ and $BC1CM$ are quite different.

3.4. Example 4. Asymmetric cross section B

The example considered here is a uniform beam with an asymmetric cross section as shown in Fig. 15. This example was studied in [22] for boundary conditions $BC1CM$. The geometry and material properties are given in Fig. 15. The section constants are as follows: $A = 2.85 \times 10^{-2} m^2$, $I_y = 1.02858 \times 10^{-3} m^4$, $I_z = 2.39265 \times 10^{-3} m^4$, $J = 2.28750 \times 10^{-6} m^4$, $I_\omega = 9.26333 \times 10^{-5} m^6$.

The lowest 14 natural frequencies of the present study together with those given in [22] are shown in Table 4. In Table 4, (A) denotes that the natural frequency corresponds to an uncoupled axial vibration. It can be seen that the agreement between the natural frequencies of the present study and those given in [22] is very good. The coupling characteristics of the

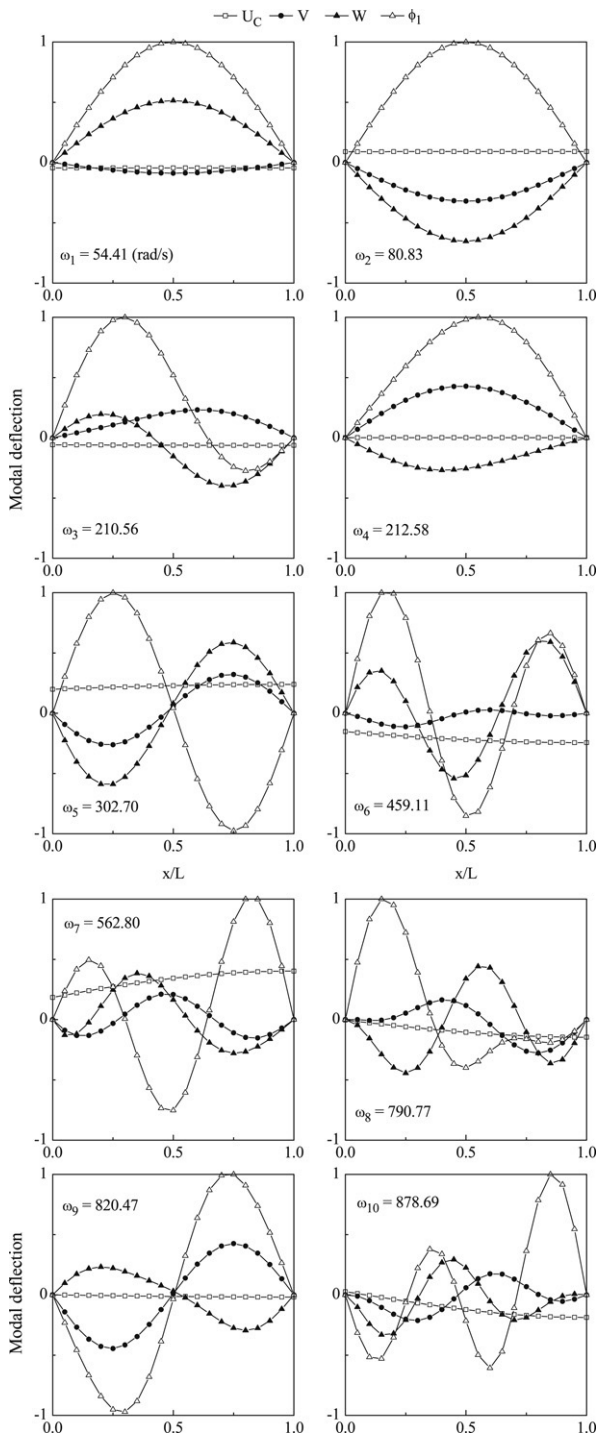

Fig. 10. The first 10 vibration mode shapes for example 3 ($BC1P$).

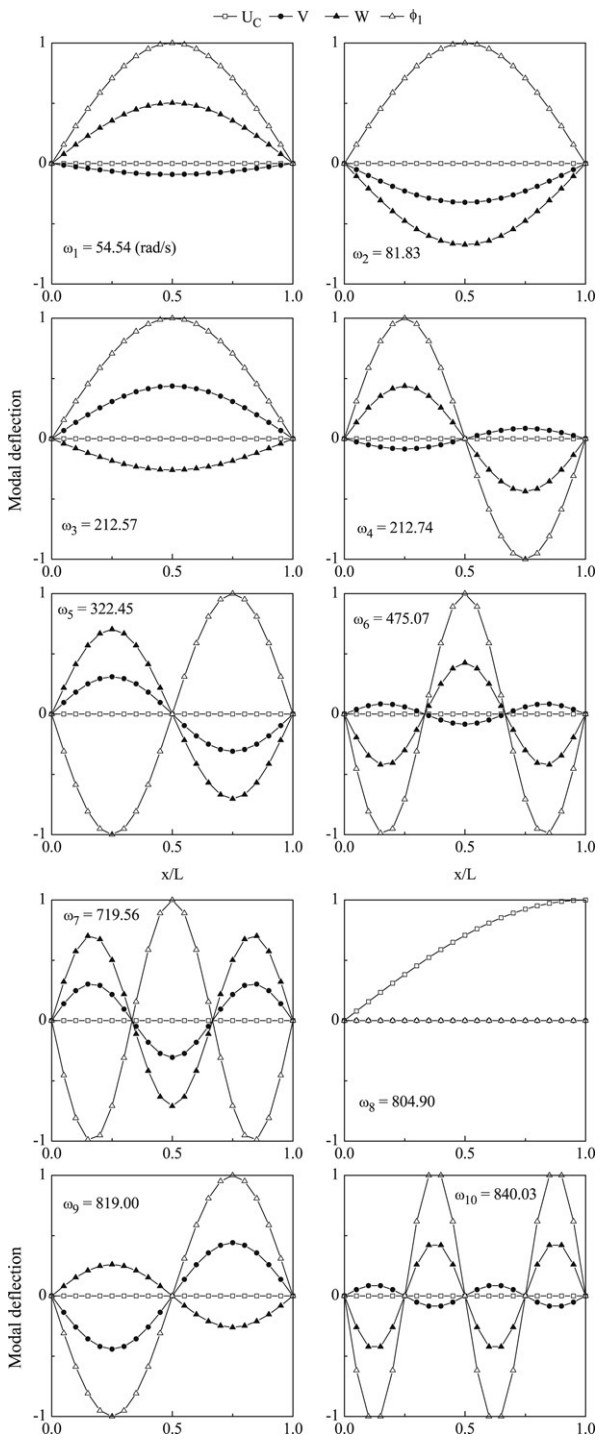

Fig. 11. The first 10 vibration mode shapes for example 3 ($BC1CM$).

free vibrations of this example are the same as those of example 3 for all boundary conditions.

3.5. Example 5. Asymmetric cross section C

The example considered here is a uniform beam with an asymmetric cross section as shown in Fig. 16. This example was studied in [22] for boundary conditions $BC1CM$. The geometry and material properties are given in Fig. 16. The section constants are as follows: $A = 2.4 \times 10^{-2}m^2$, $I_y = 6.65827 \times 10^{-4}m^4$, $I_z = 1.82139 \times 10^{-4}m^4$, $J = 5.20000 \times 10^{-6}m^4$, $I_\omega = 3.94255 \times 10^{-6}m^6$.

The lowest 12 natural frequencies of the present study together with those given in [22] are shown in Table 5. In Table 5, (A) denotes that the natural frequency corresponds to the uncoupled axial vibration. It can be seen that the agreement between the natural frequencies of the present study and those given in [22] is very good. The coupling characteristics of the

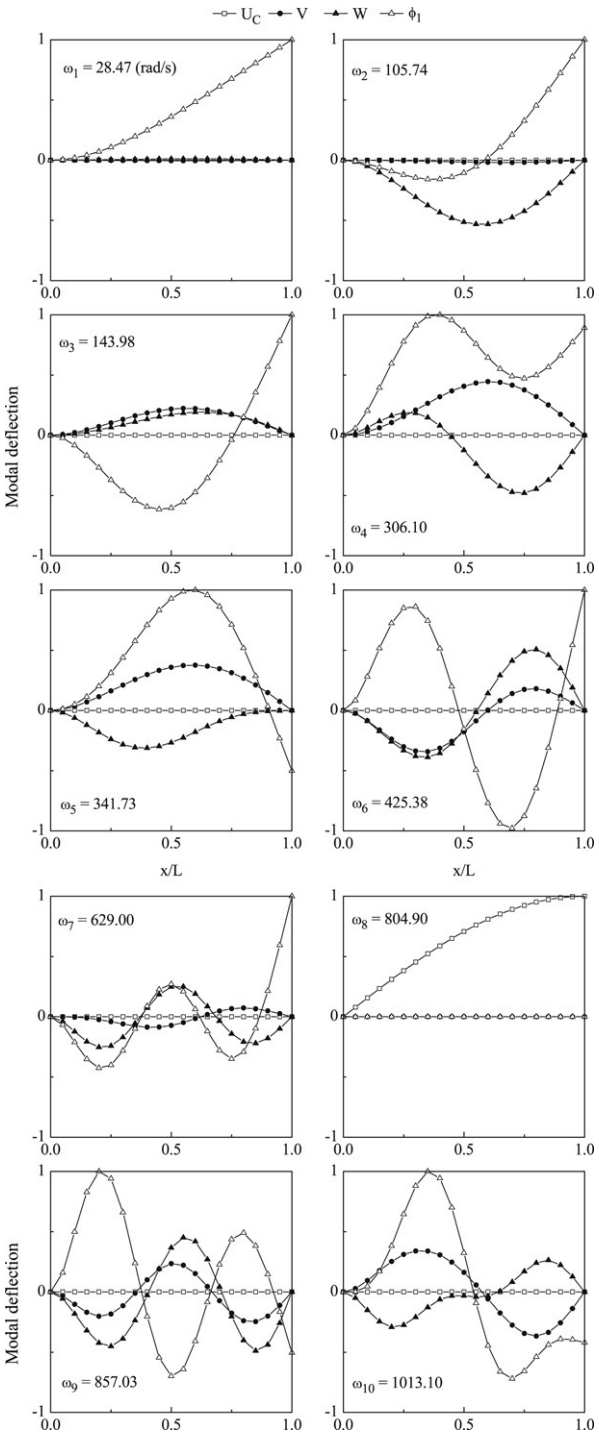

Fig. 12. The first 10 vibration mode shapes for example 3 ($BC4P$).

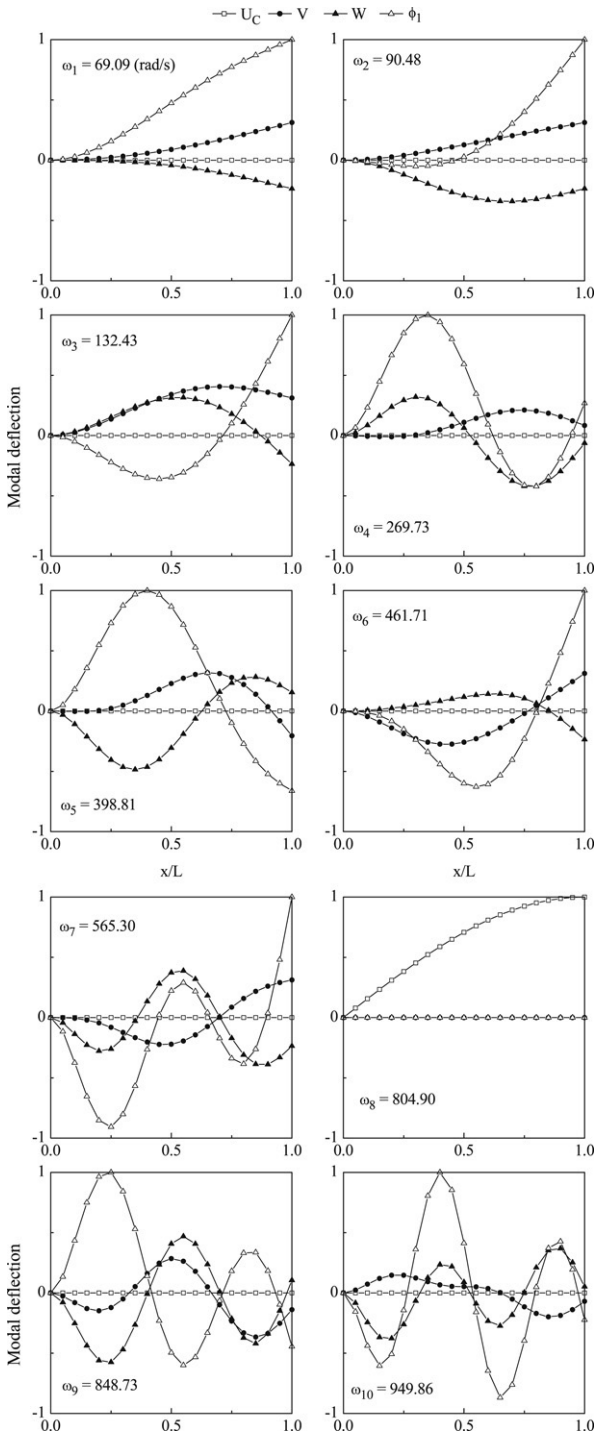

Fig. 13. The first 10 vibration mode shapes for example 3 ($BC4C$).

free vibrations of this example are the same as those of example 3 for all boundary conditions.

4. Conclusions

A finite element formulation for the coupled vibration analysis of thin-walled beams with a generic open section is presented. If the axial displacement of the pin end is restrained at any point rather than at the centroid of the asymmetric cross section, the axial vibration, two bending vibrations, and torsional vibration may all be coupled. Such a coupled vibration is induced by the boundary conditions and called a quadruply coupled vibration in the study. The element developed here has two nodes with seven degrees of freedom per node. The shear center axis is chosen to be the reference axis, and the element nodes are chosen to be located at the shear centers of the end cross sections of the beam element. Both the element deformation and inertial

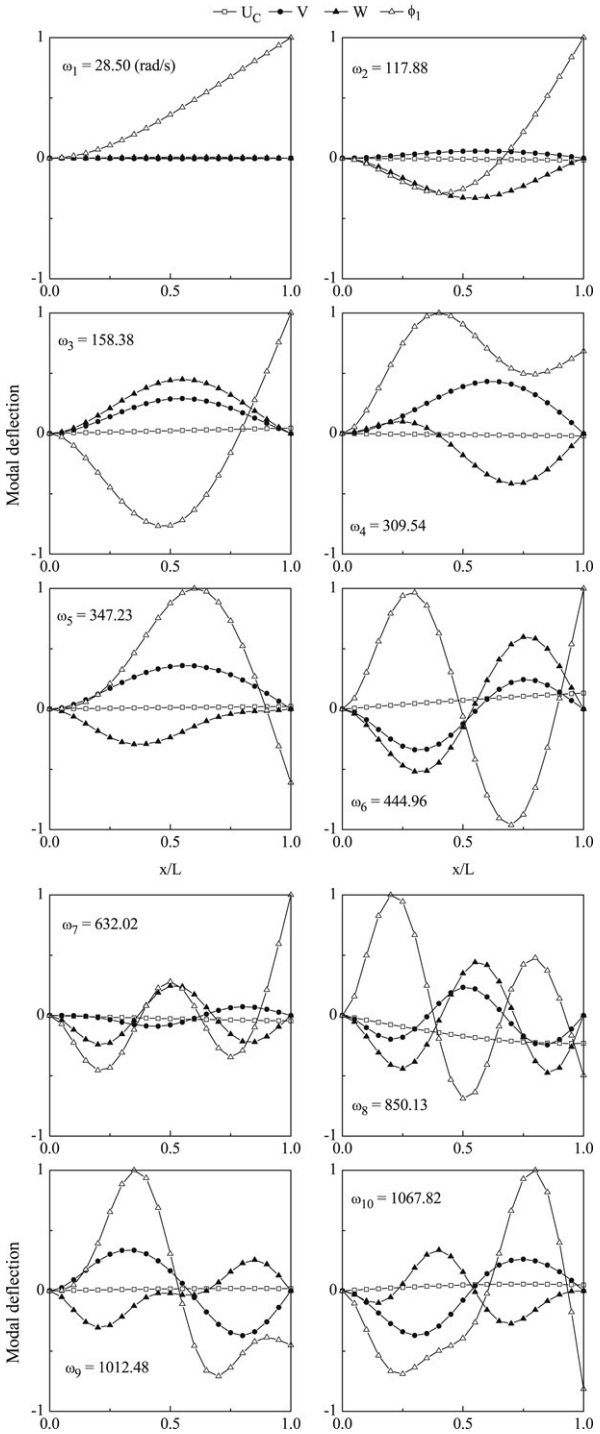

Fig. 14. The first 10 vibration mode shapes for example 3 ($BC5P$).

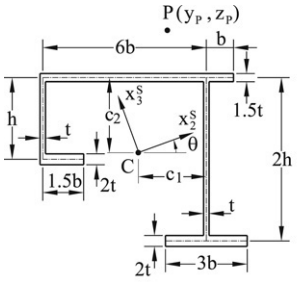

θ = −0.73487 rad
b = 0.1 m
h = 0.3 m
t = 0.01 m
c_1 = 0.21053 m
c_2 = 0.23684 m
y_P = −0.19755 m
z_P = 0.39183 m
L = 10 m
E = 210 GPa
G = 80.7 GPa
ρ = 8.002 kN·s²/m⁴

Fig. 15. Asymmetric cross section B for example 4.

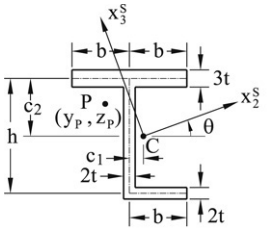

θ = 0.22839 rad
b = 0.2 m
h = 0.4 m
t = 0.01 m
c_1 = 0.01667 m
c_2 = 0.13333 m
y_P = −0.054809 m
z_P = 0.086555 m
L = 10 m
E = 210 GPa
G = 80.7 GPa
ρ = 8.002 kN·s²/m⁴

Fig. 16. Asymmetric cross section C for example 5.

nodal forces are systematically derived using a consistent first-order linearization of the exact kinematics of the Euler beam, the d'Alembert principle, and the virtual work principle. The element stiffness matrix and mass matrix are obtained by differentiating the element deformation nodal force vector and element inertial nodal force vector with respect to the element nodal parameters and their second time derivatives, respectively. To describe the restrained nodal degrees of freedom at boundaries correctly, the restrained nodal degrees of freedom at boundaries and the corresponding element nodal degrees of freedom should be identical or equivalent. Different sets of element nodal degrees of freedom corresponding to different pin ends are considered here. The relation between element matrices corresponding to different sets of element nodal degrees of freedom is derived.

From the numerical examples studied, the accuracy of the proposed method is demonstrated and the effects of different boundary conditions on the coupled vibrations of thin-wall beams are investigated. The quadruply coupled vibration of monosymmetric and asymmetric beams induced by the boundary conditions is verified.

It should be noted that the vibration can be nonlinear for slender beams. It seems that the proposed finite element formulation can be easily extended to the nonlinear vibration, if the element deformation and inertial nodal forces are derived using a consistent second-order linearization instead of the first-order linearization used here.

Table 2
Natural frequencies (rad/s) of example 2 (monosymmetric T section)

Mode	$BC1P$	$BC1CM(C)$	$BC1RM(R)$	$BC2X$	$BC3X$	$BC4P(QM)$	$BC4C$
1	190.81 (V, T)	190.81 (V, T)	190.41	78.42 (V, T)	244.89 (V, T)	121.84 (V, T)	156.50 (V, T)
2	401.87 (V, T)	401.87 (V, T)	397.83	173.56 (V, T)	506.32 (V, T)	350.98 (V, T)	310.67 (V, T)
3	463.22 (V, T)	463.22 (V, T)	462.89	287.48 (W)	727.93 (V, T)	502.69 (V, T)	473.28 (V, T)
4	729.54 (V, T)	729.54 (V, T)	729.24	351.24 (V, T)	807.18 (V, T)	655.50 (V, T)	727.28 (V, T)
5	798.98 (A,W)	804.87 (W)	798.49	582.34 (V, T)	1070.44 (V, T)	887.49 (V, T)	881.16 (V, T)
6	1007.27 (V, T)	1007.27 (V, T)	1007.00	809.52 (V, T)	1384.71 (V, T)	1182.30 (V, T)	1121.10 (V, T)
7	1303.76 (V, T)	1303.76 (V, T)	1263.67	891.15 (V, T)	1721.10 (V, T)	1256.35 (W)	1256.35 (W)
8	1336.60 (V, T)	1336.60 (V, T)	1303.94	1183.18 (V, T)	1822.37 (W)	1484.51 (V, T)	1371.65 (V, T)
9	1623.85 (V, T)	1623.85 (V, T)	1623.62	1488.77 (V, T)	2029.95 (V, T)	1667.83 (V, T)	1677.43 (V, T)
10	1971.33 (V, T)	1971.33 (V, T)	1970.92	1777.21 (W)	2089.05 (V, T)	1833.24 (V, T)	1936.55 (V, T)
Mode	$BC4R$	$BC5P$	$BC5CM$	$BC5RM$	$BC5C$	$BC5R$	
1	154.12 (V, W, T)	121.84 (V, T)	121.84 (V, T)	122.68	156.50 (V, T)	166.21	
2	338.89 (V, W, T)	350.98 (V, T)	350.98 (V, T)	356.33	310.67 (V, T)	339.36	
3	496.27 (V, W, T)	502.69 (V, T)	502.69 (V, T)	574.02	473.28 (V, T)	540.24	
4	618.64 (V, W, T)	655.50 (V, T)	655.50 (V, T)	689.69	727.28 (V, T)	673.71	
5	807.37 (V, W, T)	887.49 (V, T)	887.49 (V, T)	888.50	881.16 (V, T)	810.48	
6	1066.81 (V, W, T)	1182.30 (V, T)	1182.30 (V, T)	1182.68	1121.10 (V, T)	1069.60	
7	1328.38 (V, W, T)	1308.43 (A,W)	1256.35 (W)	1283.12	1256.35 (W)	1337.62	
8	1564.34 (V, W, T)	1484.51 (V, T)	1484.51 (V, T)	1491.44	1371.65 (V, T)	1564.74	
9	1668.21 (V, W, T)	1667.83 (V, T)	1667.83 (V, T)	1795.80	1677.43 (V, T)	1764.65	
10	1820.23 (V, W, T)	1833.24 (V, T)	1833.24 (V, T)	1834.54	1936.55 (V, T)	1866.42	

$X = P, CM, RM, C, R$.

Table 3
Natural frequencies (rad/s) of example 3 (asymmetric section A)

Mode	$BC1P$	$BC1CM(C)$	$BC1CM$ [22]	$BC2X$	$BC3X$	$BC4P(CM)$	$BC4C$	$BC5P$	$BC5CM$	$BC5C$
1	54.41	54.54	54.54	20.56	120.71	28.47	69.09	28.50	28.47	69.09
2	80.83	81.83	81.83	30.27	183.35	105.74	90.48	117.88	105.74	90.48
3	210.56	212.57	212.57	79.36	330.70	143.98	132.43	158.38	143.98	132.43
4	212.58	212.74	212.73	120.46	474.68	306.10	269.73	309.54	306.10	269.73
5	302.70	322.45	322.45	181.25	502.33	341.73	398.81	347.23	341.73	398.81
6	459.11	475.07	475.05	331.20	645.27	425.38	461.71	444.96	425.38	461.71
7	562.80	719.56	719.57	462.95	977.56	629.00	565.30	632.02	629.00	565.30
8	790.77	804.90 (A)	N/A	501.21	1061.68	804.90 (A)	804.90 (A)	850.13	857.03	848.73
9	820.47	819.00	819.01	644.42	1269.75	857.03	848.73	1012.48	1013.10	949.86
10	878.69	840.03	N/A	804.90 (A)	1577.75	1013.10	949.86	1067.82	1072.85	1216.53
11	1293.13	1267.51	N/A	972.67	1601.13	1072.85	1216.53	1223.76	1431.19	1433.88
12	1333.75	1305.48	N/A	1059.01	1611.04 (A)	1431.19	1433.88	1570.27	1570.48	1459.15
13	1767.33	1768.81	1768.75	1241.30	2190.78	1570.48	1459.15	1598.39	1611.04 (A)	1611.04 (A)

$X = P, CM, C$.

Table 4
Natural frequencies (rad/s) of example 4 (asymmetric section B)

Mode	$BC1P$	$BC1CM(C)$	$BC1CM$ [22]	$BC2X$	$BC3X$	$BC4P(CM)$	$BC4C$	$BC5P$	$BC5CM$	$BC5C$
1	51.04	51.05	51.05	19.90	112.22	21.28	62.42	21.28	21.28	62.42
2	99.54	101.41	101.41	36.28	229.58	111.88	96.20	112.36	111.88	96.20
3	197.75	197.83	197.83	84.57	307.25	158.91	160.30	187.16	158.91	160.30
4	233.55	233.71	233.71	112.35	526.86	306.30	255.80	306.43	306.30	255.80
5	364.98	402.91	402.91	225.30	599.54	365.52	461.10	365.98	365.52	461.10
6	441.26	441.50	441.48	307.98	628.53	509.63	510.88	533.23	509.63	510.88
7	625.25	780.81	N/A	509.03	986.80	599.04	557.20	599.04	599.04	557.20
8	781.51	804.90 (A)	N/A	599.06	1219.46	804.90 (A)	804.90 (A)	978.02	981.20	893.59
9	904.06	897.70	897.74	624.98	1402.48	981.20	893.59	1011.03	1054.73	1053.95
10	994.17	904.15	904.15	804.90 (A)	1467.33	1054.73	1053.95	1141.47	1142.01	1281.91
11	1214.69	1214.04	N/A	984.82	1611.04 (A)	1142.01	1281.91	1372.70	1461.92	1403.15
12	1582.53	1574.92	N/A	1209.22	1988.18	1461.92	1403.15	1465.25	1611.04 (A)	1611.04 (A)
13	1738.79	1739.13	N/A	1362.38	2038.97	1776.45	1779.76	1899.29	1776.45	1779.76
14	1937.23	1940.05	1939.99	1463.16	2616.21	2029.51	1905.92	2029.77	2029.51	1905.92

$X = P, CM, C$.

Table 5
Natural frequencies (rad/s) of example 5 (asymmetric section C)

Mode	$BC1P$	$BC1CM(C)$	$BC1CM$ [22]	$BC2X$	$BC3X$	$BC4P(CM)$	$BC4C$	$BC5P$	$BC5CM$	$BC5C$
1	42.40	42.41	42.41	15.48	84.94	39.24	45.81	39.29	39.24	45.81
2	74.87	74.91	74.91	29.18	127.94	74.36	67.39	76.10	74.36	67.39
3	99.46	99.48	99.48	47.64	203.43	126.16	120.76	127.88	126.16	120.76
4	150.81	150.87	150.87	92.68	213.46	148.00	163.45	148.38	148.00	163.45
5	226.73	227.12	227.12	148.38	331.36	222.28	209.18	223.13	222.28	209.18
6	304.69	304.82	304.81	203.39	392.35	290.06	306.11	291.46	290.06	306.11
7	356.92	357.86	357.85	232.31	553.67	405.22	376.53	405.22	405.22	376.53
8	472.06	474.66	474.64	342.04	624.20	453.38	472.62	454.64	453.38	472.62
9	508.53	508.85	N/A	409.06	632.79	550.77	555.65	552.01	550.77	555.65
10	739.28	766.58	N/A	553.95	910.30	644.14	641.19	644.15	644.14	641.19
11	768.56	792.11	792.13	627.93	1031.86	804.90 (A)	804.90 (A)	891.55	891.86	856.82
12	804.26	804.90 (A)	N/A	649.16	1073.95	891.86	856.82	925.77	926.92	925.45

$X = P, CM, C$.

Acknowledgements

The authors would like to acknowledge the constructive and thoughtful comments of the referees.

References

[1] Mei C. Coupled vibrations of thin-walled beams of open section using the finite element method. Int J Mech Sci 1970;12:883–91.
[2] Hallauer WL, Liu RYL. Beam bending–torsion dynamic stiffness method for calculation of exact vibration modes. J Sound Vib 1982;85(1):105–13.
[3] Friberg PO. Coupled vibrations of beams—an exact dynamic element stiffness matrix. Int J Numer Methods Eng 1983;19:479–93.
[4] Friberg PO. Beam element matrices derived from Vlasov's theory of open thin-walled elastic beams. Int J Numer Methods Eng 1985;21:1205–28.
[5] Dokumaci E. An exact solution for coupled bending and torsion vibrations of uniform beams having single cross-sectional symmetry. J Sound Vib 1987;119(3):443–9.
[6] Bishop RED, Cannon SM, Miao S. On coupled bending and torsional vibration of uniform beams. J Sound Vib 1989;131:457–64.
[7] Banerjee JR. Coupled bending–torsional dynamic stiffness matrix for beam elements. Int J Numer Methods Eng 1989;28:1283–98.
[8] Leung AYT. Natural shape functions of a compressed Vlasov element. Thin-Walled Struct 1991;11:431–8.
[9] Banerjee JR, Fisher SA. Coupled bending–torsional dynamic stiffness matrix for axially loaded beam elements. Int J Numer Methods Eng 1992; 33:739–51.
[10] Klausbruckner MJ, Pryputniewicz RJ. Theoretical and experimental study of coupled vibrations of channel beams. J Sound Vib 1995;183(2):239–52.
[11] Banerjee JR, Williams FW. Clamped-clamped natural frequencies of a bending–torsion coupled beam. J Sound Vib 1994;176(3):301–6.
[12] Banerjee JR, Guo S, Howson WP. Exact dynamic stiffness matrix of a bending–torsion coupled beam including waring. Comput Struct 1996; 59(4):613–21.
[13] Yaman Y. Vibrations of open-section channels: A coupled flexural and torsional. J Sound Vib 1997;204(1):131–58.
[14] Kim SB, Kim MY. Improved formulation for spatial stability and free vibration of thin-walled tapered beams and space frames. Eng Struct 2000; 22:446–58.
[15] Matsui Y, Hayashikawa T. Dynamic stiffness analysis for torsional vibration of continuous beams with thin-walled cross-section. J Sound Vib 2001;243(2):301–16.
[16] Arpaci A, Bozdag E. On free vibration analysis of thin-walled beams with nonsymmetrical open cross-sections. Comput Struct 2002;80:691–5.
[17] Kim MY, Yun HT, Kim NI. Exact dynamic and static element stiffness matrices of nonsymmetric thin-walled beam–columns. Comput Struct 2003;81:1425–48.
[18] Arpaci A, Bozdag SE, Sunbuloglu E. Triply coupled vibrations of thin-walled open-section beams including rotary inertia effects. J Sound Vib 2003;260:889–900.
[19] Li J, Shen R, Hua H, Jin X. Coupled bending and torsional vibration of axially loaded Bernoulli–Euler beams including warping effects. Appl Acoust 2004;65:153–70.
[20] Li J, Li W, Shen R, Hua H. Coupled bending and torsional vibration of nonsymmetrical axially loaded thin-walled Bernoulli–Euler beams. Mech Res Commun 2004;31:697–711.
[21] Mohri F, Azrar L, Potier-Ferry M. Vibration analysis of buckled thin-walled beams with open sections. J Sound Vib 2004;275:434–46.
[22] Prokic A. On triply coupled vibrations of thin-walled beams with arbitrary cross-section. J Sound Vib 2005;279:723–37.
[23] Gökdağ H, Kopmaz O. Coupled bending and torsional vibration of a beam with in-span and tip attachments. J Sound Vib 2005;287:591–610.
[24] Sapountzakis EJ, Tsiatas GC. Flexural–torsional vibrations of beams by BEM. Comput Mech 2007;39:409–17.
[25] Prokić A. On fivefold coupled vibrations of Timoshenko thin-walled beams. Eng Struct 2006;28:54–62.
[26] Chen HH, Lin WY, Hsiao KM. Co-rotational finite element formulation for thin-walled beams with generic open section. Comput Methods Appl Mech Eng 2006;195:2334–70.
[27] Cook RD, Young WC. Advanced mechanics of materials. New York: Macmillan Publishing Company; 1985.
[28] Sapountzakis EJ. Solution of non-uniform torsion of bars by an integral equation method. Comput Struct 2000;77:659–67.
[29] Sapountzakis EJ, Mokos VG. Nonuniform torsion of composite bars by boundary element method. J Eng Mech, ASCE 2001;127(9):945–53.
[30] Hsiao KM. Corotational total Lagrangian formulation for three-dimensional beam element. AIAA J 1992;30:797–804.
[31] Hsiao KM, Lin JY, Lin WY. A consistent co-rotational finite element formulation for geometrically nonlinear dynamic analysis of 3-D beams. Comput Methods Appl Mech Eng 1999;169:1–18.
[32] Chung TJ. Continuum mechanics. New Jersey: Prentice-Hall; 1988.
[33] Bathe KJ. Finite element procedure in engineering analysis. New Jersey: Prentice-Hall; 1982.